Geol. Mag. **147** (*4*), *2010, pp. 527–550. © Cambridge University Press 2010*
doi:10.1017/S0016756809990835

Geochemical and palynological study of the Upper Famennian Dasberg event horizon from the Holy Cross Mountains (central Poland)

LESZEK MARYNOWSKI, PAWEŁ FILIPIAK* & MICHAŁ ZATOŃ

University of Silesia, Faculty of Earth Sciences, Będzińska Str. 60, 41-200 Sosnowiec, Poland

(*Received* 14 May 2009; *accepted* 26 November 2009; First published online 15 January 2010)

Abstract – Integrated palynological, organic and inorganic geochemical and petrographical methods have been used for deciphering the depositional redox conditions and character of organic matter of the Famennian Dasberg event horizon from the deep-shelf Kowala succession of the Holy Cross Mountains. The ages of the investigated samples have been established, using miospore data, as VF (*Diducites versabilis–Grandispora famenensis*) and LV (*Retispora lepidophyta–Apiculiretusispora verrucosa*) miospore Zones of the Middle/Upper Famennian. In the standard conodont zonation, this corresponds to the uppermost *postera* to lowermost *praesulcata* Zones. The presence of green sulphur bacteria biomarkers and dominance of small-sized framboids together with the presence of large framboids and low values of the U/Th ratio may indicate that during sedimentation of the lower Dasberg shale, intermittent anoxia occurred in the water column, or the anoxic conditions prevailed in the upper part of the water column, while the bottom waters were oxygenated, at least briefly. Deposition of the upper Dasberg shale was characterized by both bottom water and water column anoxia. The lack of acritarcha taxa from these intervals could have been due to anoxia in the photic zone. Moreover, organic content is high in those samples. There is no geochemical evidence for anoxia during sedimentation of the deposits sandwiched between the lower and upper Dasberg shales, or in the deposits which underlie and overlie both Dasberg shale horizons. The two discrete anoxic events are interpreted to be the result of major transgressions and the blooming of primary producers. Above the Dasberg shales, small fragments of charcoal and raised concentrations of polycyclic aromatic hydrocarbons are detected. This supports the presence of wildfires during deposition of shales just above the boundary of VF/LV palynological zones. Temperatures calculated from the fusinite reflectance values suggest that the charcoal was formed in low-temperature ground and/or surface fires. The typical marine character of sedimentation combined with the high proportion of charcoals suggests that wildfires were large-scale, and that there was intensive transport of terrestrial material. The main causes of intensive wildfires were a significant rise of O_2 in the atmosphere and important progress in the land plant diversity during Late Devonian times. Palynofacies studies suggest that the transgression corresponds to the part IIf of the Late Devonian sea-level curve.

Keywords: Dasberg event, photic zone euxinia, isorenieratane, palynology, palynofacies, charcoal, wildfires, PAHs, Holy Cross Mountains.

1. Introduction

The Late Devonian is an epoch which saw significant changes in the biosphere. For instance, the Frasnian/Famennian boundary (F/F) extinction was one of the five most important events during Phanerozoic times. The Devonian–Carboniferous Hangenberg event represents one of the largest biotic disturbances (for reviews, see House, 2002; Caplan & Bustin, 1999). Late Devonian global events, such as the *punctata* event (Pisarzowska, Sobstel & Racki, 2006; Yans *et al.* 2007; Marynowski, Filipiak & Pisarzowska, 2008), Lower and Upper Kellwasser (F/F) events (Joachimski *et al.* 2001; Racki *et al.* 2002; Bond & Zatoń, 2003; Bond, Wignall & Racki, 2004; Hartkopf-Fröder *et al.* 2007; Bond & Wignall, 2008), the *Annulata* event (Marynowski, Narkiewicz & Grelowski, 2000; Bond & Zatoń, 2003; Racka & Marynowski, 2008) or the Hangenberg event (Marynowski & Filipiak, 2007; Trela & Malec, 2007) are relatively well recognized from the palaeontological and geochemical points of view in the Holy Cross Mountains. All are characterized by the presence of organic-rich deposits, particularly distinctive black shale horizons (*sensu* Wignall, 1994), with elevated concentrations of organic carbon, in some cases exceeding 20 % of total organic carbon (TOC). The Dasberg event, known as a worldwide hypoxic event (Hartenfels & Becker, in press, and references therein), has been relatively little studied. The present work is a continuation of the multidisciplinary research (geochemistry and palynology) concerning development and environmental perturbations recorded in Upper Devonian black shale (Hangenberg and Dasberg) exposed on the northern wall of the Kowala Quarry (see Fig. 1; Filipiak & Racki, 2005; Racki, 2005; Marynowski & Filipiak, 2007).

*Author for correspondence: filipiak@us.edu.pl

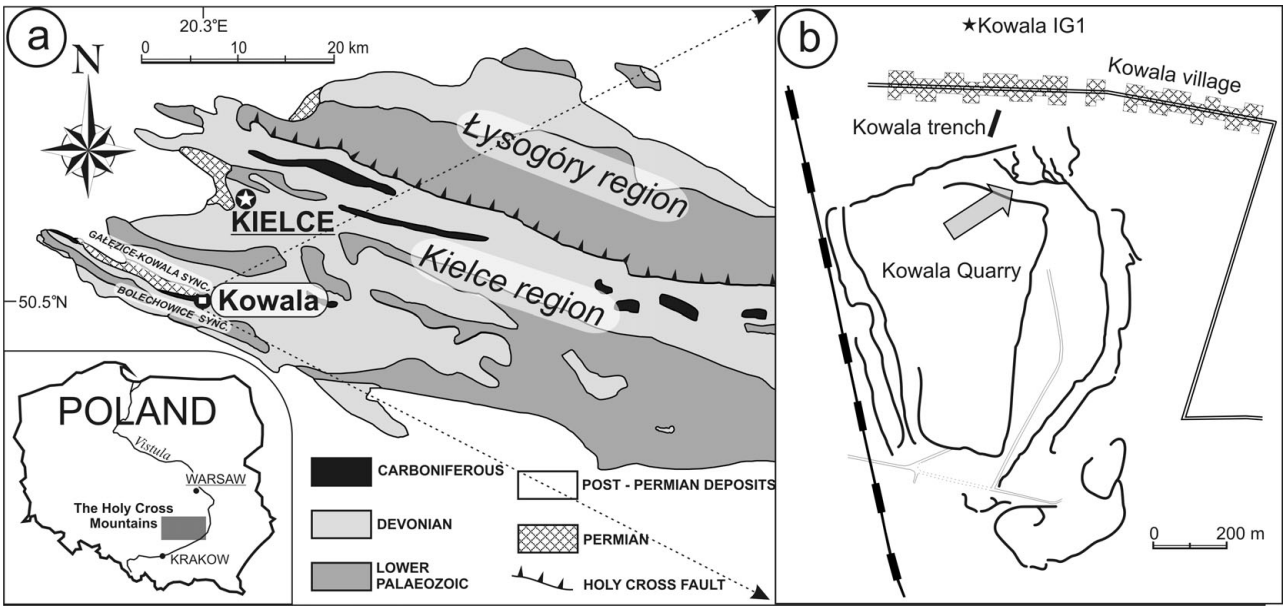

Figure 1. Simplified geological map of the western and central part of the Holy Cross Mountains (a) with location of the Kowala Quarry (b).

Here we report the first palynological (palynostratigraphy and palynofacies) and geochemical study of the Upper Devonian Dasberg Event section (Fig. 2), especially focused on depositional environments in the Holy Cross Mountains (HCM) area (Fig. 1). The study is particularly interesting due to the immature character of the organic matter (OM) in the Kowala quarry section (Racki, 2005). The relative immaturity of Devonian sedimentary rocks provides an insight into a wide range of sedimentary and biotic aspects which enrich our knowledge of Palaeozoic events. The results have been compared to other Late Devonian event intervals recorded in the Holy Cross Mountains such as the F/F event (Joachimski *et al.* 2001), D/C (Marynowski & Filipiak, 2007) and the Early–Middle Frasnian transitions (Marynowski, Filipiak & Pisarzowska, 2008).

2. Geological setting

The well-known large active Kowala Quarry is geologically located in the southern limb of the Gałęzice–Kowala syncline of the Holy Cross Mountains (Fig. 1) (see e.g. Racki *et al.* 2002). Because detailed data concerning the previous stratigraphical and lithological studies of the deep-shelf (basinal) Kowala section have already been presented by Marynowski & Filipiak (2007), in the present paper we have described only the lithology of the currently analysed part of the section (Fig. 2a, b). Lithological divisions of the Famennian sequence have been presented by, for example, Szulczewski (1971) and Berkowski (2002), and stratigraphical data come mainly from Żakowa, Nehring-Lefeld & Malec (1985), Turnau (1990) and Dzik (1997, 2006).

2.a. Lithology and lithostratigraphy

The currently analysed part of the Middle/Upper Famennian section at Kowala belongs to sets K and L (Szulczewski, 1971; Berkowski, 2002). Generally, its lithology consists of a rhythmic succession of marly shales, marly limestones and limestones distinctly intercalated with two black shale horizons (Fig. 2a, b).

Above two metres of light grey limestones rhythmically intercalated with darker marly shales, a lower black shale horizon (~ 55 cm thick), divided into two parts, characterizes an abrupt sedimentary change (Fig. 2b). A nodular limestone parting, 10 cm thick, is visible sandwiched between the black shale. Above this, one metre of another package of rhythmically, thinly bedded limestones and marly shales occurs. It is overlain by a much thinner (~ 4 cm in thickness), upper black shale horizon. The first, thicker and stratigraphically older black shales, divided by nodular limestone into two parts, are an equivalent of the internationally known Dasberg Event horizon (Fig. 2).

2.b. Dasberg Shales (DBS) in Western Europe: similarities and differences

The most comprehensive data on the lithological development and biostratigraphy of the DBS have been recently presented by Hartenfels & Becker (in press) from the European and North African areas. During bed by bed investigation of several sections, they established the chronostratigraphy, biostratigraphy and eustasy of the global event. Taking the lithological development into account, the sections described from the Rhenish Massif (Germany) (e.g. Effenberg and Oese) are the most similar to the Middle/Upper Famennian sequences of the Kowala Quarry. Generally, a rhythmic succession of marly limestones and marly

https://doi.org/10.1017/S0016756809990835 Published online by Cambridge University Press

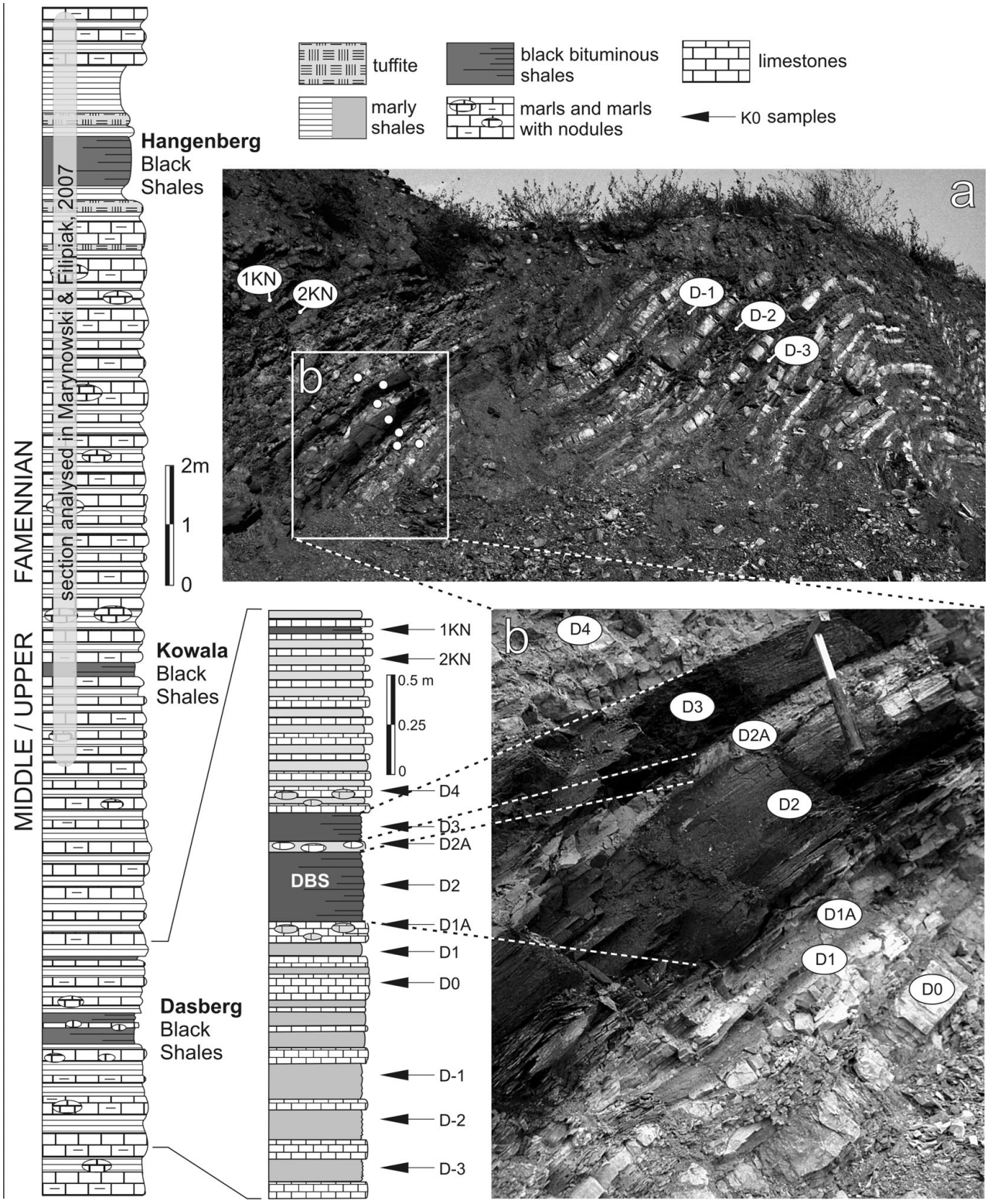

Figure 2. The general lithology of Middle/Upper Devonian section of northern wall of the Kowala Quarry, with currently analysed section enlarged. (a) View of the Dasberg part of the section and samples location (VI 2005). (b) Enlarged part of the section with Dasberg black shales and sample location.

shales with sudden occurrence of ~ 30 cm thick black shales is present in the German area. Moreover, the second, thinner (~ 5 cm thick) dark layer above the DBS in the Effenberg Quarry (Korn, 2004; Hartenfels & Becker, in press), similar to that exposed in the Kowala Quarry (Fig. 2), occurs as well. It is notable that unlike in German sections, the DBS in the Kowala Quarry is thicker (~ 55 cm) and divided into two parts by the nodular limestone layer. However, the general lithological similarities, supported by palynological data, indicate that these Famennian sediments exposed in the Kowala Quarry represent the Dasberg Event interval.

https://doi.org/10.1017/S0016756809990835 Published online by Cambridge University Press

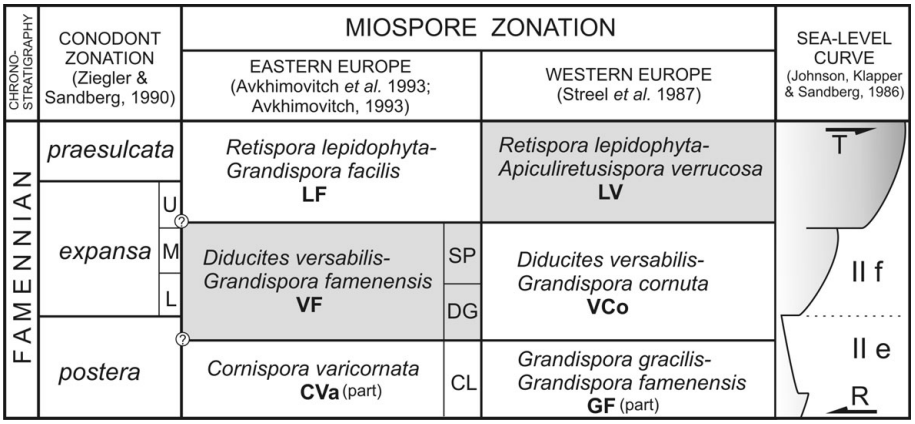

Figure 3. Correlation of the miospore and conodont zonal schemes for the Middle/Upper Famennian of western Europe and Russian Platform with the T/R curve.

Our biostratigraphical data of the section are based exclusively on miospores, which are not as precise as the conodonts or ammonoids used by Hartenfels & Becker (in press); however, a tentative correlation based on standard miospore zonation by Streel *et al.* (1987) and Avkhimovitch *et al.* (1993) indicates more or less precisely the uppermost *postera*–lowermost *praesulcata* interval in the conodont zonation (Fig. 3).

3. Materials and methods

All information about samples and methods is presented in the online Supplementary Material at http://www.cambridge.org/journals/geo.

4. Palynostratigraphy

The palynological study was conducted in order to establish a palynostratigraphical framework and to analyse the relative abundances of particular kerogen components. The two Middle/Upper Famennian miospore Zones were recognized: *Diducites versabilis–Grandispora famenensis* (VF) and *Retispora lepidophyta–Apiculiretusispora verrucosa* LV (Fig. 3). Due to changing similarities of investigated miospore assemblages to those characterizing different standard miospore zones, two miospore schemes were used. The older recognized miospore zone (VF) has been assigned to the eastern European zonation by Avkhimovitch *et al.* (1993), but the younger (LV) assemblage has been assigned to the western European scheme proposed by Streel *et al.* (1987). The assignment to a particular zone was based on the presence of the zonal index species and characteristic assemblage.

4.a. *Diducites versabilis–Grandispora famenensis* (VF) Zone

The VF miospore Zone has been recognized in the first three analysed samples D-3, D-2 and D-1 (Fig. 4). The assemblage is taxonomically diverse and contains the index species *Diducites versabilis* and *Grandispora famenensis* accompanied by *Retispora macroreticulata, Rugospora radiata, Hymenospora intertextus, Diducites poljessicus, Endoculeospora gradzinskii* and *Grandispora facilis* (Fig. 5). Additionally, in the sample D-2, *Lophozonotriletes proscurrus* has been found, which, according to Avkhimovitch *et al.* (1993), together with *G. facilis* mentioned above, is an important taxon for the SP (*Spelaeotriletes papulosus*; the younger part of the VF Zone) Subzone in the Eastern European miospore scheme. Other, more frequent miospores noticed in this assemblage are: *Corbulispora cancellata*, *Endoculeospora setacea, Raistrickia baculata, Gorgonispora crassa, Knoxisporites hederatus* and *Cymbosporites acutus*. It is of note that *Grandispora cornuta*, the index taxon for the VCo miospore Zone for Western Europe (see Streel *et al.* 1987; Fig. 3) has been found only in sample D-1.

In addition to numerous terrestrial components, phytoplankton is very rich and diverse although without stratigraphical value.

4.b. *Retispora lepidophyta–Apiculiretusispora verrucosa* (LV) Zone

The LV miospore Zone has been recognized in the remaining analysed samples, from D1 to 1KN (Fig. 4). The regular occurrence of the first index species *Retispora lepidophyta* (Fig. 5) characterizes the beginning of the next LV Zone (Streel *et al.* 1987). *Apiculiretusispora verrucosa*, a nominal species, was recorded in the D1 and D1A samples only. The miospore assemblage, observed in the samples D1–D3 (Fig. 4), consists of similar species as previously observed in the proceeding VF Zone: *Retispora macroreticulata, Grandispora facilis, G. famenensis, Diducites mucronatus, D. versabilis, D. poljessicus, Endoculeospora gradzinskii, E. setacea* and *Hymenospora intertextus* (Fig. 5). Generally, *Diducites* spp. and *Grandispora* spp. are the most common taxa among miospores recorded in this level. According to Avkhimovitch *et al.* (1993) and the previous results (Filipiak, 2004), the last occurrence of *Hymenospora intertextus* is noted at the top of the VF Zone, while this taxon is constantly present here, together with 'younger' *Retispora lepidophyta* (D1–D3 samples;

https://doi.org/10.1017/S0016756809990835 Published online by Cambridge University Press

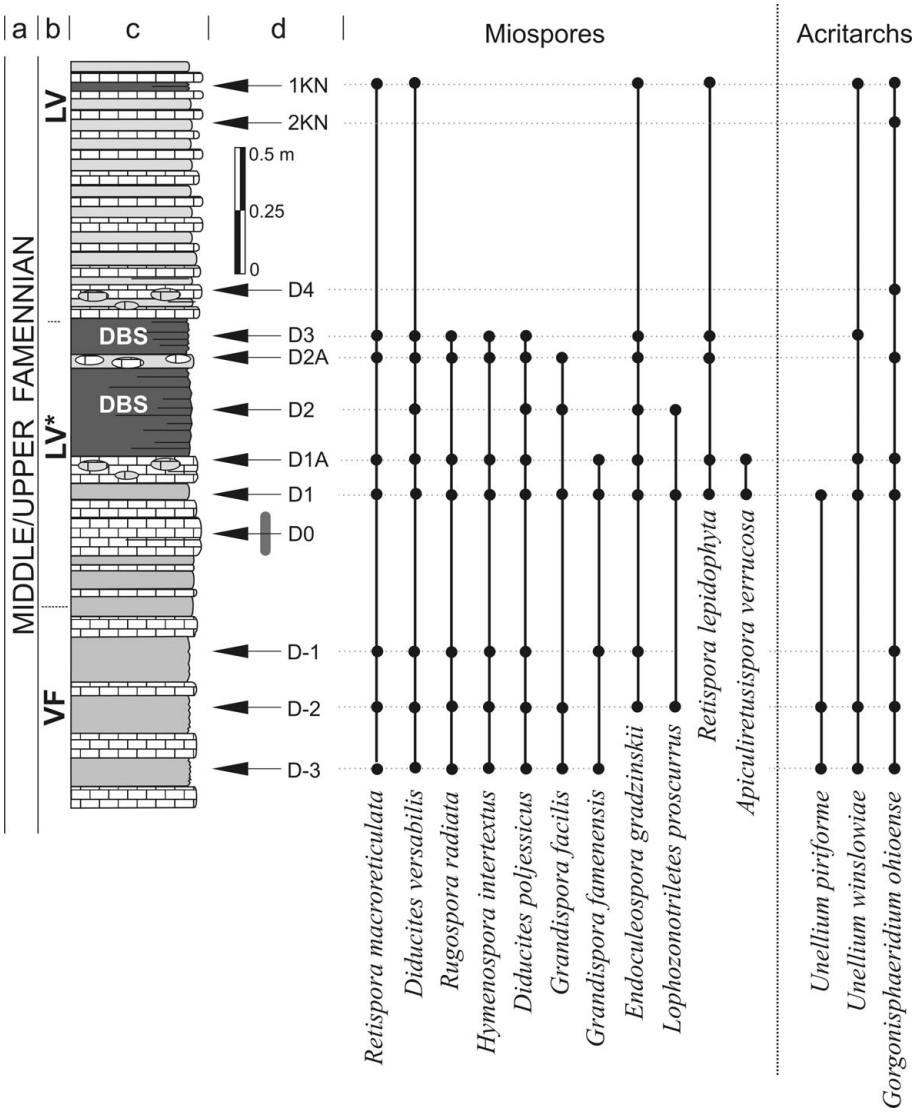

Figure 4. Stratigraphical range of important miospore and acritarcha species (for lithology explanations see Fig. 2). a – chronostratigraphy; b – palynostratigraphy; c – lithological section; d – samples. LV* indicates a transitional interval to the typical LV Zone.

Fig. 4). The very rare presence of both index species *Retispora lepidophyta* and *Apiculirtusispora verrucosa* (< 1 %) and constant occurrence of *Hymenospora intertextus* may indicate that between samples D1 and D3 there is a 'transitional interval' (named LV* here; see Fig. 4) between the typical VF and LV miospore Zones. The typical LV miospore Zone (but without *A. verrucosa*) has been identified in the last two analysed samples (1KN and 2KN). However, it is notable that samples from the upper part of the analysed section (D4–1KN) are poorer in taxa and generally possess miospore assemblages that are less diversified (see Fig. 4). The *echinata* Subzone (the youngest part of the LV Zone) was previously recognized in this section (see fig. 4 in Marynowski & Filipiak, 2007), five metres above the currently investigated samples (Fig. 2).

The organic remains are rich in phytoplankton as well but without stratigraphical value. Among the acritarch taxa, *Gorgonisphaeridium ohioense* is the most common. The frequent occurrence of this species has been noticed previously by Filipiak (2005) and Marynowski & Filipiak (2007) at the same LV biostratigraphical level.

5. Palynofacies

5.a. Observations

Countable kerogen components have been divided into four categories. Acritarchs together with prasinophytes and leiospheres indicate a marine environment, but miospores and plant tracheids are land-derived (e.g. Batten, 1996). Leiospheres, as distinct and very common palynomorphs, are excluded from the rest of the prasinophyta group and treated as a separate component here. The relative abundance of acritarchs, along with prasinophytes (Figs 6, 7), and versus miospores, is distinctly variable in the investigated succession, especially when comparing its lowermost and upper parts.

https://doi.org/10.1017/S0016756809990835 Published online by Cambridge University Press

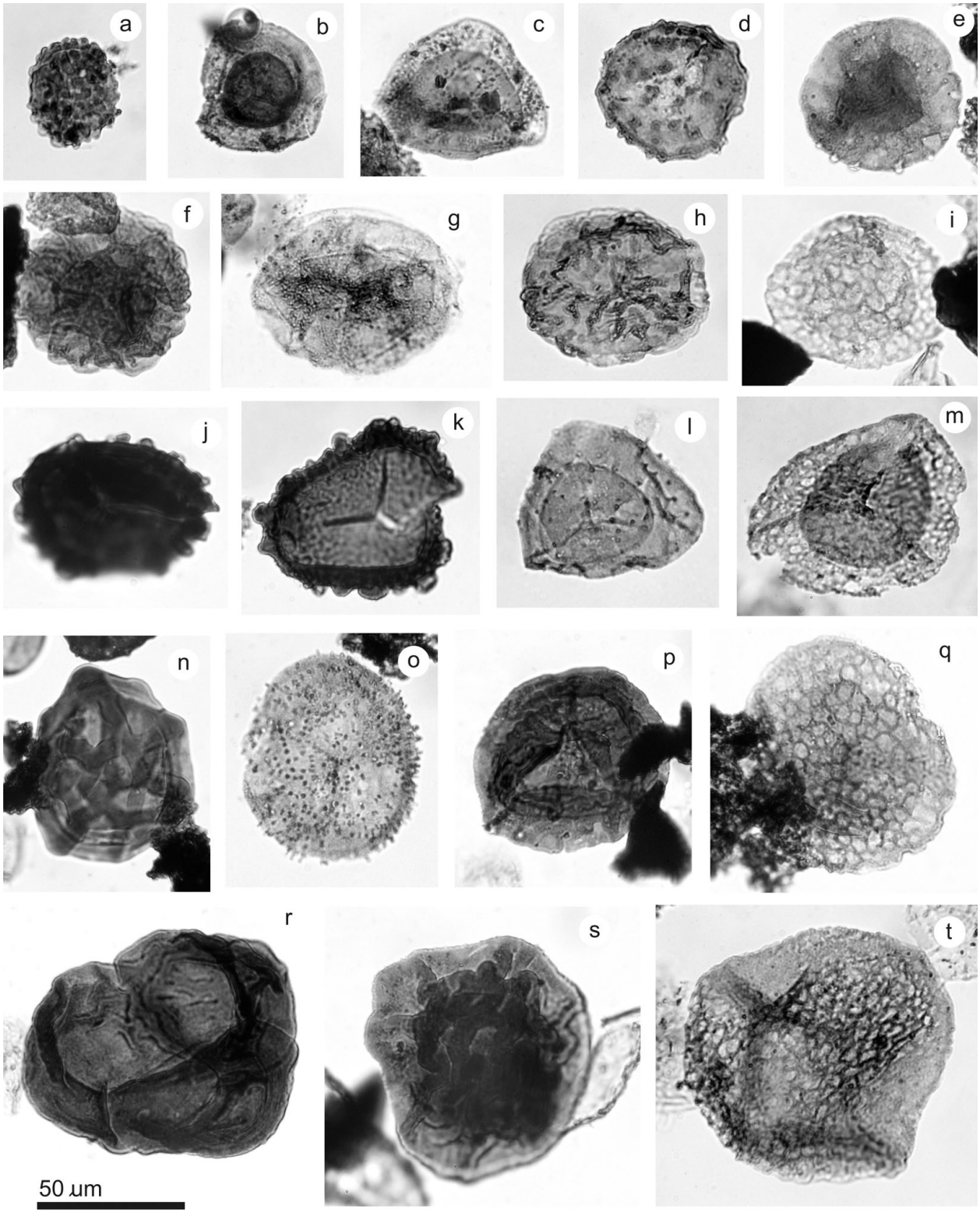

Figure 5. Famennian miospores (VF-LV Zones). (a) *Lophozonotriletes proscurrus* Kedo. Kowala sample D1. (b) *Spelaeotriletes papulosus* (Sennova) Avkhimovitch. Kowala sample D-3. (c) *Endoculeospora gradzinskii* Turnau, 1975. Kowala D-1. (d) *Grandispora famenensis* Streel, 1974 (*in* Becker *et al*. 1974). Kowala sample D-3. (e) *Diducites mucronatus* (Kedo) Van Veen, 1981. Kowala sample D1A. (f) *Diducites versabilis* (Kedo) Van Veen, 1981. Kowala sample D-3. (g) *Diducites poljessicus* (Kedo) Van Veen, 1981. Kowala sample D1. (h) *Rugospora radiata* (Jushko) Byvscheva 1985. Kowala sample D-3. (i) *Retispora lepidophyta* (Kedo) Playford, 1976. Kowala sample D1. (j) *Raistrickia baculata* Filipiak, 1996. Kowala sample D-3. (k) *Raistrickia baculata* Filipiak, 1996. Kowala sample D1A. (l) *Grandispora facilis* (Kedo) Avkhimovitch, 1988 (*in* Avkhimovitch *et al.* 1988). Kowala sample D1. (m) *Retispora lepidophyta* (Kedo) Playford, 1976. Kowala sample D2A. (n) *Knoxisporites dedaleus* (Naumova) Moreau-Benoit, 1980. Kowala sample D-3. (o) *Endoculeospora setacea* (Kedo) Avkhimovitch & Higgs, 1988 (*in* Avkhimovitch *et al.* 1988). Kowala sample D-3. (p) *Hymenospora intertextus* (Nekriata & Sergeeva) Avkhimovitch & Loboziak, 1993 (*in* Avkhimovitch *et al.* 1993). Kowala sample D2A. (q) *Retispora lepidophyta?* (Kedo) Playford, 1976 or *R. macroreticulata?* (Kedo) Byvscheva, 1985. Kowala sample D1A. (r) Miospore tetrad. Kowala sample D-3. (s) *Hymenospora intertextus* (Nekriata & Seergeeva) Avkhimovitch & Loboziak, 1993 (*in* Avkhimovitch *et al.* 1993). (t) *Retispora macroreticulata* (Kedo) Byvscheva, 1985. Kowala sample D-3.

https://doi.org/10.1017/S0016756809990835 Published online by Cambridge University Press

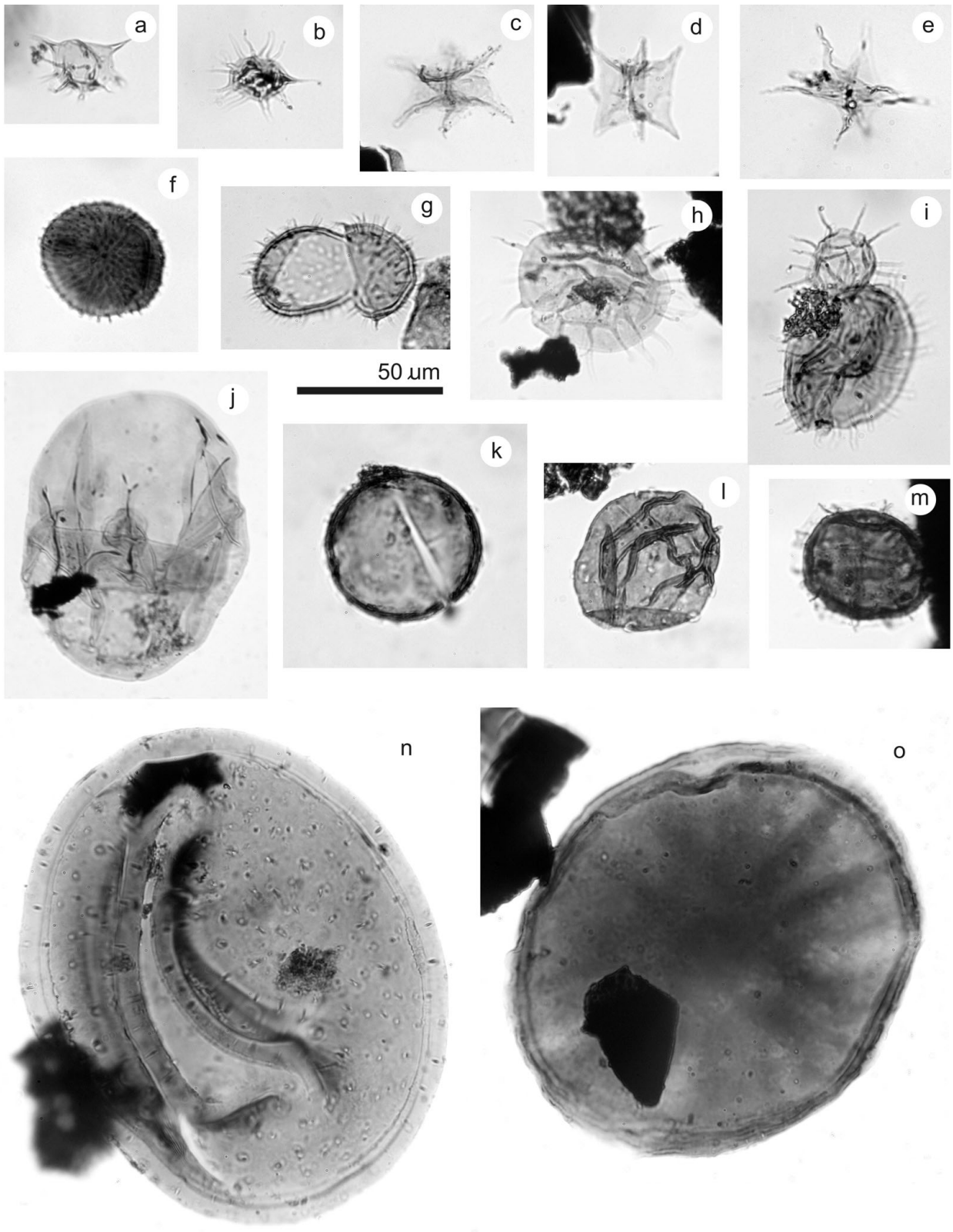

Figure 6. Famennian phytoplankton. (a) *Unellium winslowiae* Rauscher, 1969. Kowala sample D1. (b) *Unellium* cf. *piriforme* Rauscher, 1969. Kowala sample D-3. (c) *Polyedryxium pharaone* Deunf, 1961. Kowala sample 2KN. (d) *Veryhachium polyester* Staplin, 1961. Kowala sample 2KN. (e) *Stellinium micropolygonale* (Stockmans & Willière) Playford, 1977. Kowala sample D-3. (f) *Gorgonisphaeridium discissum* Playford, 1981 (*in* Playford & Dring, 1981). Kowala sample 2KN. (g) *Gorgonisphaeridium* sp. Kowala sample D-3. (h) *Gorgonisphaeridium ohioense* (Winslow) Wicander, 1974. Kowala sample 1KN. (i) *Solisphaeridium*(?) sp. and *Gorgonisphaeridium ohioense* (Winslow) Wicander, 1974. Kowala sample 2KN. (j) *Leiosphaeridia* sp. Kowala sample D1. (k) *Hemiruptia* sp. Kowala sample 1KN. (l) *Leiosphaeridia* sp. Kowala sample D1A. (m) *Cymatiosphaera perimembrana* Staplin, 1961. Kowala sample 2KN. (n) *Tasmanites* sp. Kowala sample 1KN. (o) *Maranhites mosesii* (Sommer) González, 2009. Kowala sample 2KN.

https://doi.org/10.1017/S0016756809990835 Published online by Cambridge University Press

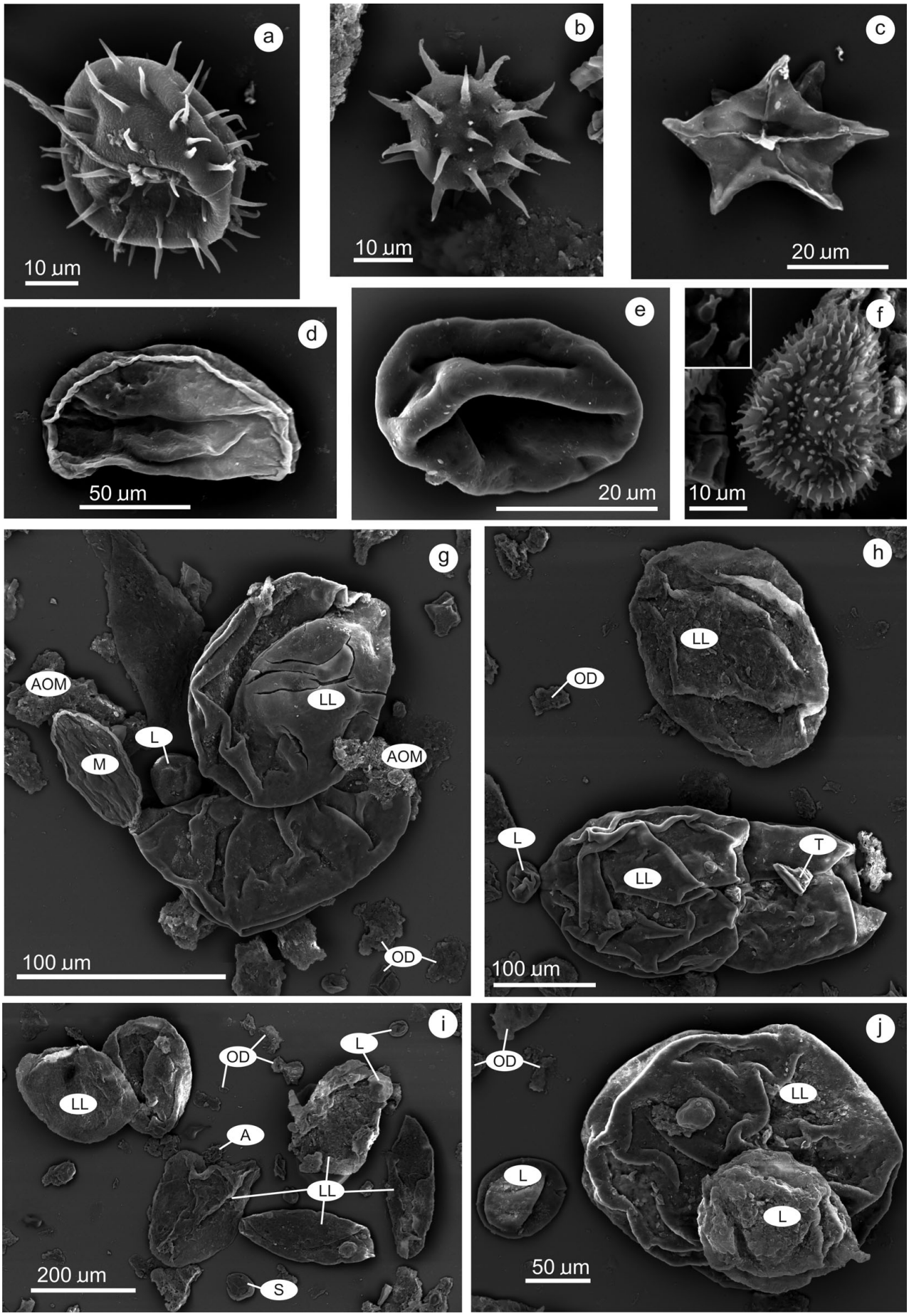

Figure 7. For caption see facing page.

https://doi.org/10.1017/S0016756809990835 Published online by Cambridge University Press

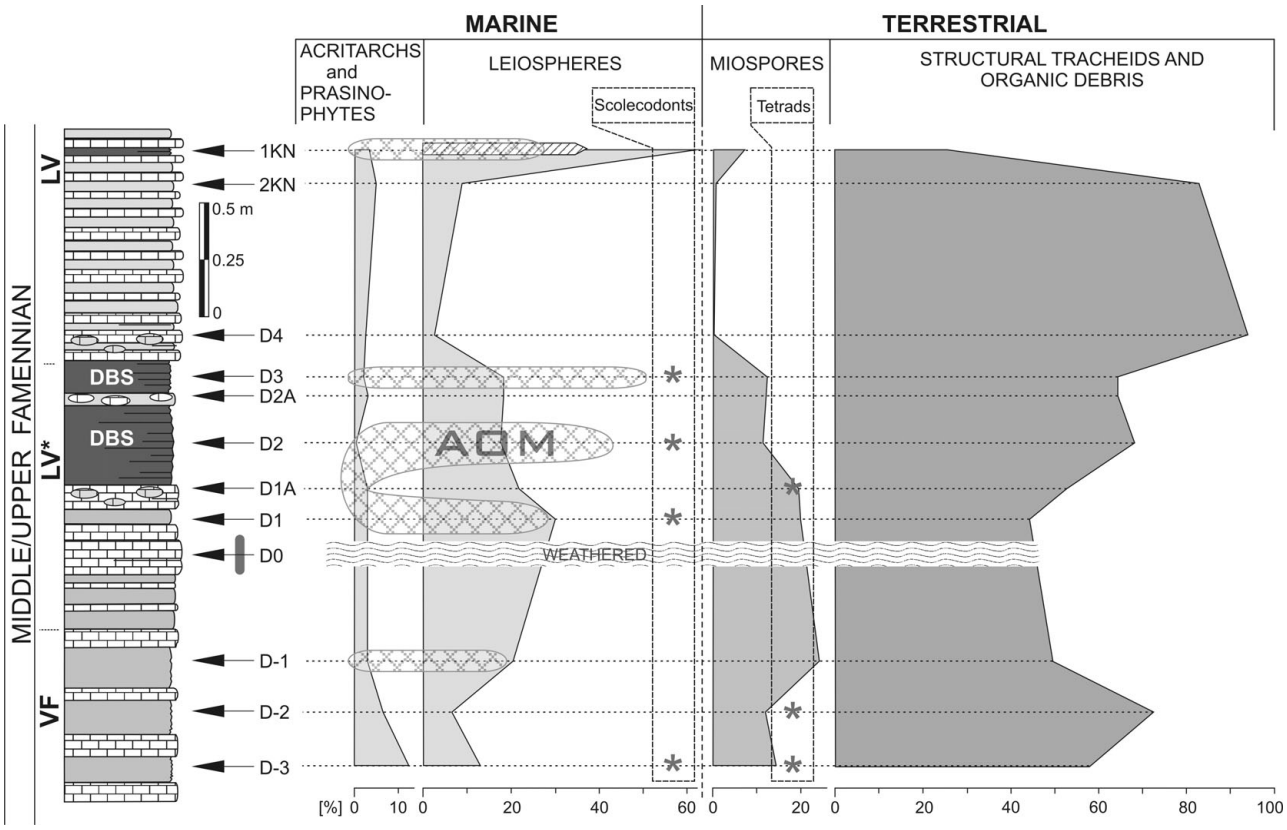

Figure 8. Percentages of kerogen components and abundance of AOM (amorphous organic matter). The dashed area (1KN sample) indicates presences of leiospheres larger than 180 μm.

Detailed relative changes among the above mentioned components are compiled in Figure 8, but a more precise description of the palynofacies component fluctuations is in the online Supplementary Material at http://www.cambridge.org/journals/geo.

5.b. Palynofacies interpretation

Taking into account the proportions of various components of the palynofacies, we may suggest that depositional conditions changed slightly with time from a more inshore to offshore environment in the Chęciny–Zbrza intrashelf basin (e.g. Racki *et al.* 2002). Excluding three topmost samples, within the thin black shale at the top of the section (1KN), there is no sharp change in palynofacies composition between the DBS and the rest of the underlying samples. Generally, the amount of terrestrial particles (Fig. 9) is smaller here. However, this could be connected with a deepening phase of the basin and/or diluting effect connected with a great amorphous organic matter (AOM) content (Tyson, 1993; Chow, Wendte & Stasiuk, 1995; Fig. 10). The main difference between palynofacies of the DBS (sample D2) and those from the other samples is a complete lack of acritarchs and the smaller-sized leiospheres in the DBS (Figs 8, 10). Thanks to the present geochemical analysis (Fig. 11) it is clear that DBS sedimentation prevailed under anoxic or even euxinic conditions in the water column, which probably restricted phytoplankton growth (mostly acritarchs) in a stressed habitat (e.g. Habib & Knapp, 1982). The common occurrence of prasinophytes, even in oxygen-depleted environments, can be explained by their presumed green algal nature (e.g. Tappan, 1980; Tyson, 1995). Possessing chlorophyll, they could have thrived in the near-surface photic zone of the sea (Guy-Ohlson, 1996), far above the unfavourable environmental conditions, in which no other planktic biota could have thrived. Thus, blooming of prasinophycean algae and their subsequent deposition in the greater depths are regarded as good indications of a stressed environment. On the other hand, however, prasinophytes are also more tolerant of stressful conditions than other phytoplankton (Tappan, 1982; Hartkopf-Fröder *et al.* 2007).

Figure 7. Environmental scanning electron microscope photo of phytoplankton and palynofacies. (a) *Gorgonisphaeridium ohioense* (Winslow) Wicander, 1974. Kowala sample 1KN. (b) *Micrhystridium stellatum* Deflandre, 1945. Kowala sample 1KN. (c) *Stellinium micropolygonale* (Stockmans & Willière) Playford, 1977. Kowala sample 2KN. (d) *Maranhites mosesii* (Sommer) González, 2009. Kowala sample 1KN. (e) *Leiosphaeridia* sp. Kowala sample 2KN. (f) *Gorgonisphaeridium discissum* Playford, 1981 (*in* Playford & Dring, 1981); the small picture in the left upper corner shows ornamentation details. Kowala sample 2KN. (g–j) Palynofacies from the Kowala 1KN sample composed mainly by *Leiosphaeridia* (L), large *Leiosphaeridia* (LL) with small amount of miospores (S), *Maranhites* (M), acritarchs (A), plant tracheid (T), amorphous organic matter (AOM) and organic debris (OD).

https://doi.org/10.1017/S0016756809990835 Published online by Cambridge University Press

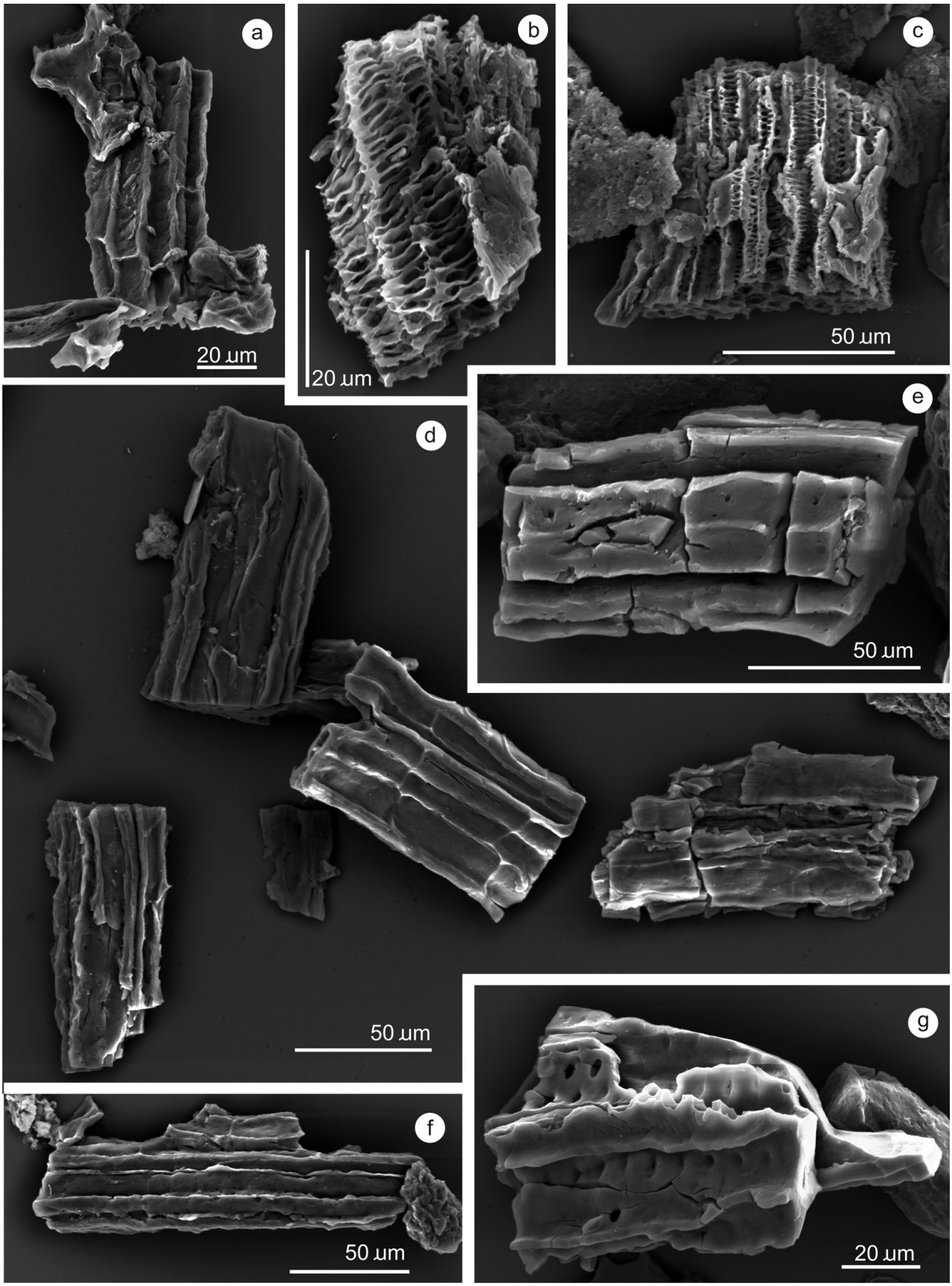

Figure 9. Environmental scanning electron microscope photo of charcoal. (a, b, d–g) Kowala sample 2KN; (c) Kowala sample 1KN; internal cellular structure perfectly preserved (see, for example, a–c, g).

https://doi.org/10.1017/S0016756809990835 Published online by Cambridge University Press

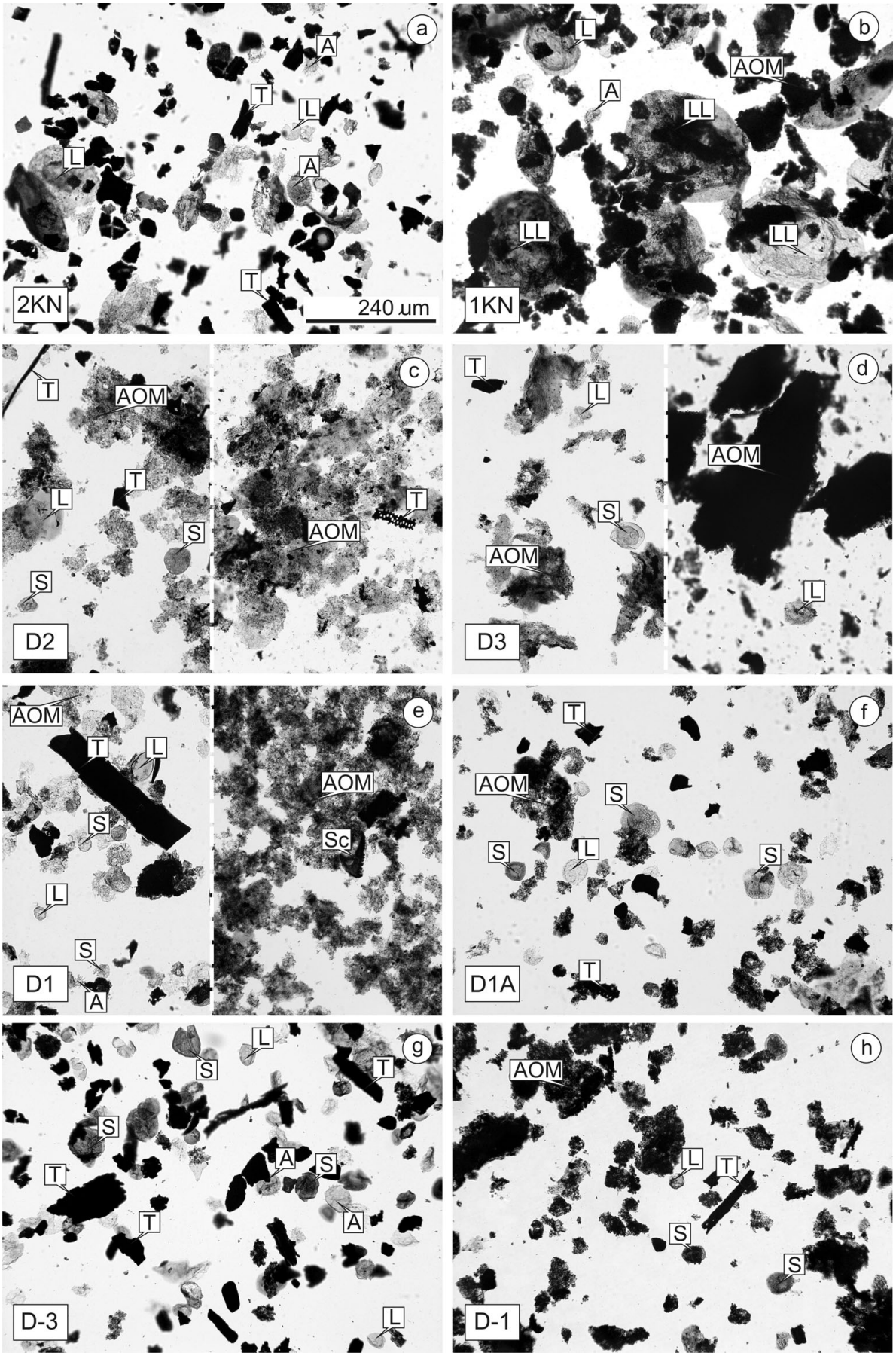

Figure 10. Transmitted light microscope pictures of eight selected palynofacies. In the lower left corner is the sample code. Dashed lines divide some picture (c–e) on two parts. On the right side is palynofacies before HNO_3 treatment, on the left the same sample after AOM partly removed. Abbreviations: A – acritarcha, AOM – amorphic organic matter, L – leiosphere, LL – large leiosphere (> 180 µm), S – miospore, Sc – scolecodont, T – tracheid.

https://doi.org/10.1017/S0016756809990835 Published online by Cambridge University Press

Table 1. Bulk geochemical data, percentage yields of fractions and basic molecular parameters

Sample	TOC (%)	Carb (%)	EOM (mg/g TOC)	T_{max} (°C)	HI (mgHC/g TOC)	OI ($mgCO_2$/g TOC)	Fractions AL (%)	Fractions AR (%)	Fractions POL (%)	$CPI_{(25–31)}$	Pr/Ph	Pr/nC_{17}	Ph/nC_{18}	SCh/LCh
1 KN	3.21	18.03	15	–	–	–	15	29	56	1.27	4.73	2.44	0.50	3.80
2 KN	0.63	26.50	15	–	–	–	42	16	42	1.07	0.57	0.74	0.79	0.69
D 4	0.19	37.29	35	–	–	–	19	29	52	1.49	0.71	0.82	0.68	4.57
D 3	15.44	26.29	48	419	388	36	14	26	60	1.07	1.53	8.22	6.87	3.76
D 2A	0.48	48.50	23	433	23	141	29	21	50	1.22	2.57	2.16	0.74	4.86
D 2	9.14	30.92	67	416	428	27	9	24	67	1.09	1.80	8.58	5.89	3.54
D 1A	0.27	46.92	54	–	–	–	28	6	66	1.27	1.27	1.17	0.64	4.45
D 1	4.58	32.12	26	431	190	74	18	16	66	1.15	3.89	5.61	1.62	4.69
D 0	0.03	85.02	55	–	–	–	18	23	59	1.50	0.60	0.98	0.81	3.01
D -2	1.74	34.25	13	–	–	–	19	14	67	1.20	3.34	3.07	0.88	6.04
D -3	1.51	31.10	17	–	–	–	22	10	68	1.25	2.90	2.20	0.90	5.84

TOC – total organic carbon; Carb – carbonates; EOM – extractable organic matter; HI – hydrogen index; OI – oxygen index; AL – aliphatic, AR – aromatic, POL – polar; CPI – carbon preference index; Pr – pristane; Ph – phytane; SCh/LCh – short chain to long chain *n*-alkanes ratio: $(nC_{17}+nC_{18}+nC_{19})/(nC_{27}+nC_{28}+nC_{29})$.

Their phycoma permits survival under unfavourable conditions, such as a lack of sunlight, or other environmental/hydrochemical changes, such as anoxia (see Tyson, 1995). Data have also been retrieved from the upper part of the section (D4–2KN) and from the second thinner black shale horizon (1KN). The relative high amount of tracheids in samples D4 and 2KN, together with decreasing amount of similarly land-derived miospores, indicates rather offshore conditions during sedimentation and can be connected with a transgression episode (e.g. Summerhayes, 1987; Tyson, 1993). This hypothesis is supported by the more taxonomically differentiated marine phytoplankton present in samples from this part of the section. According to Johnson, Klapper & Sandberg (1986), the transgression began at the base of the Lower *expansa* conodont Zone, known as an initiation of the IIf cycle on the Euramerican sea-level curve (see Fig. 3).

In the last sample (1KN), phytoplankton is the most differentiated, rich in thick-walled and large species of *Leiosphaeridia, Maranhites* and *Tasmanites* (Figs 6, 7, 10) with more limited terrestrial components indicating a more open marine environment, characterized by suitable trophic conditions, which could have enhanced bio-productivity. Similar large forms of sphaeromorphs have previously been observed from the F/F boundary interval (Filipiak, 2002) and from the Middle Frasnian strata (Filipiak *in* Marynowski, Filipiak & Pisarzowska, 2008) in the Kowala succession. In those intervals their elevated amount was connected with a positive carbon isotopic anomaly (Joachimski *et al.* 2001; Racki *et al.* 2002; Pisarzowska, Sobstel & Racki, 2006). The biogeochemical perturbations could indicate exceptionally favourable environmental conditions, increasing nutrient supply for phytoplankton growth (Joachimski *et al.* 2001; Yans *et al.* 2007). The slight decrease in terrestrial components is generally observed in samples possessing AOM concentration. According to Tyson (1993), the percentage of terrestrial organic matter particles is strongly dependent on AOM concentration. In cases where AOM and prasinophytes are well-preserved and richly present, terrestrial components are usually significantly diluted. It is interesting that three samples possessing high concentrations of AOM (D1, D2 and D3; Fig. 10) yield scolecodonts as well (see Fig. 8). However, the abundance of AOM is strongly correlated with areas of low bottom-water oxygen content (Tyson, 1993). Then, the infrequent scolecodonts present in dysoxic–anoxic deposits (e.g. samples D1, D2 and D3) may be explained by their secondary origin, such as from fish fecal pellets (Tyson, 1995), or they are the remains of some polychaete annelids that were well-adapted to an oxygen-depleted environment (Courtinat, 1998). The miospore tetrads appear rather infrequently as single elements, especially in samples from the lower part of the investigated section (D-2 and D-3), and they are completely absent in all samples from the top of the section. It is obvious that their presence generally increases landward, because they are heavier and often most abundant closer to the parental flora sources (Tyson, 1993).

In summary, all palynofacies components, especially those from the three topmost samples (D4–1KN), show relative changes connected to a progressive deepening (Johnson, Klapper & Sandberg, 1986). Generally, the currently analysed palynofacies demonstrate rather small changes in composition of the phytoplankton community from the DBS and underlying strata. The main difference concerns the complete lack of acritarchs in the D2 sample with the constant presence of leiosphere 'disaster' taxa (Tappan, 1986), which can be interpreted as an effect of anoxia in the water column. The large sizes of prasinophyta in the 1KN sample can most probably be explained by the onset of favourable trophic ocean conditions (Marynowski, Filipiak & Pisarzowska, 2008).

5.c. Comparison with the Hangenberg Black Shale

See Section 3 of online Supplementary Material text at http://www.cambridge.org/journals/geo.

6. Organic geochemistry

6.a. Bulk geochemical and petrographical data

Total organic carbon (TOC) content differs significantly between samples (Table 1, Fig. 11). Organic-poor

https://doi.org/10.1017/S0016756809990835 Published online by Cambridge University Press

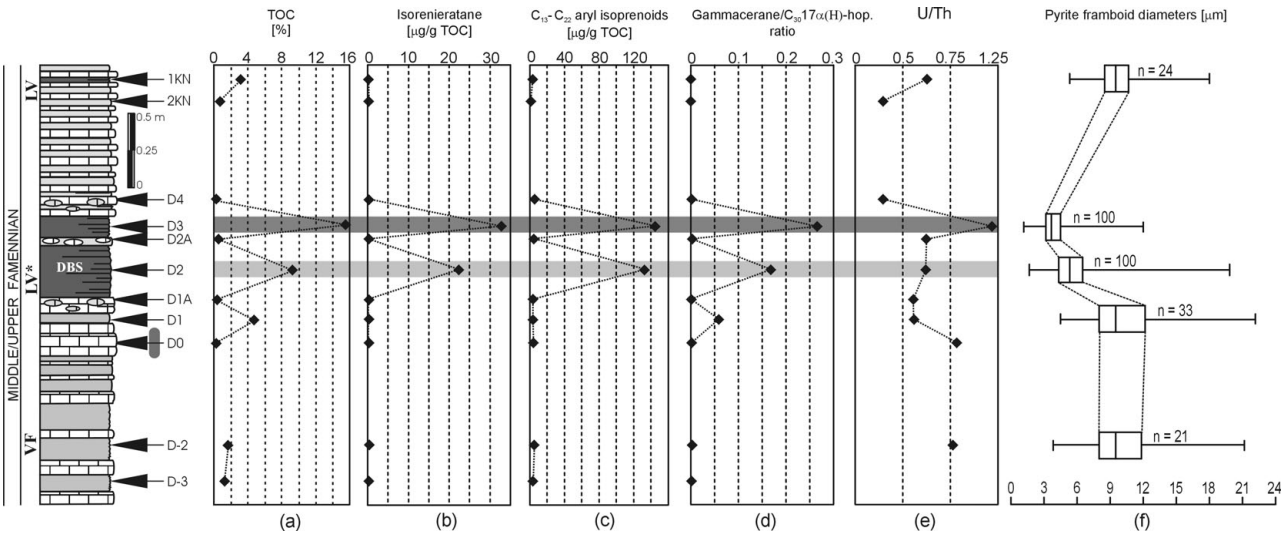

Figure 11. Composite plot of the Dasberg event section showing organic carbon, biomarkers, U/Th and pyrite analyses data. (a) Total organic carbon content – TOC (%). (b) Isorenieratane concentration (μg/g TOC). (c) C_{13}–C_{22} aryl isoprenoids concentration (μg/g TOC). (d) Gammacerane/C_{30} 17α(H)-hopane ratio. (e) Uranium/thorium (U/Th) ratio. (f) Box-and-whisker plots of the pyrite framboid diameters. Shaded levels responds to the lower and upper Dasberg black shales.

limestones and marls (samples D0, D1A, D2A and D4) contain 0.03 to 0.48 % TOC (Table 1). Some marls, marly shales and greenish shales contained an average TOC amount (D-2, D-3 and 2KN) ranging from 0.63 to 1.74 % TOC (Table 1). Two dark-grey shale samples (D1 and 1KN), characterized by relatively high TOC amounts, ranged from 3.21 to 4.58 %, and the main Dasberg black shales (D2 and D3) contain 9.14 and 15.44 % TOC, respectively (Table 1). Comparable high TOC amounts, exceeding 10 %, were noted from the Hangenberg and Kowala black shales (Marynowski & Filipiak, 2007), whereas Middle Frasnian black shales and F/F boundary shales and limestones contain generally lower TOC concentrations in the range of 0.5 to 8 % (Joachimski *et al.* 2001; Marynowski, Filipiak & Pisarzowska, 2008). Black shales (samples D2 and D3) are characterized by relatively high HI and low OI (Table 1), which is characteristic for kerogen type II (e.g. Armstroff *et al.* 2006). Such values are typical for Upper Devonian organic-rich facies from the Holy Cross Mountains (Joachimski *et al.* 2001; Marynowski & Filipiak, 2007; Marynowski, Rakociński & Zatoń, 2007).

Vitrinite and fusinite reflectance values were measured for sample 1KN in order to obtain the maturity range and compare it to the literature data, and to calculate the approximate temperature of wildfires based on fusinite reflectance (Jones & Lim, 2000).

The vitrinite reflectance values, based on measurements of 70 vitrinite particles, are identical as average values (Marynowski, Czechowski, & Simoneit, 2001), attaining 0.53 % R_r. Fusinite fragments (105 particles measured) showed a relatively wide range of reflectance values, but average values are much higher than that of vitrinite. The values range from 0.62 % to 1.88 % with mean value of 0.86 %. Calculated temperatures of charcoal formation, based on the formula presented by Jones & Lim (2000), ranged from approximately 257 to 406 °C, with a mean value of 286 °C. Some additional information on the maturity data and distribution of *n*-alkanes, isoprenoids and steroids is available in the online Supplementary Material text at http://www.cambridge.org/journals/geo.

6.b. Triterpanes

Hopanes are important constituents of the aliphatic fraction of all samples. The most abundant hopane is C_{30}-17α,21β-hopane, but in some samples, especially from the upper part of the section (1KN and 2KN), the most abundant are 17α-22,29,30-trisnorhopane (Tm) and C_{29}-17α,21β-norhopane (Fig. 12).

Values for the ratio of the βα-hopane to the sum of βα + αβ-hopane (Peters, Walters & Moldowan, 2005) in almost the total sample set are 0.29 ± 0.1, which is characteristic for low to moderately mature organic matter. Lower values (~ 0.1) were noted only for samples D0 and D1A, most probably due to their partial weathering (Elie *et al.* 2000; see also Fig. 8).

The distribution of homohopanes (C_{31} to C_{35} αβ-hopanes) differs significantly between samples. All samples are characterized by a predominance of $C_{31}(S+R)$ homologues but the presence of both $C_{35}(S+R)$ and $C_{34}(S+R)$-homohopanes was affirmed in only two black shale samples (Fig. 12). Moreover, $C_{33}(S+R)$-homohopanes are relatively abundant in the black Dasberg shales and almost absent in the rest of the samples (Fig. 12). The lack of higher molecular weight homohopanes is not typical for marine basinal samples (Marynowski, Narkiewicz & Grelowski, 2000) but much more typical for coals and terrestrial organic matter (e.g. Disnar & Harouna, 1994).

Values of hopanes/*n*-alkanes ratios for organic rich samples are comparable to those obtained for the Early–Middle Frasnian transition (Marynowski, Filipiak & Pisarzowska, 2008) and higher than for the F/F transition (Joachimski *et al.* 2001), showing enhanced bacterial and/or cyanobacterial contributions

https://doi.org/10.1017/S0016756809990835 Published online by Cambridge University Press

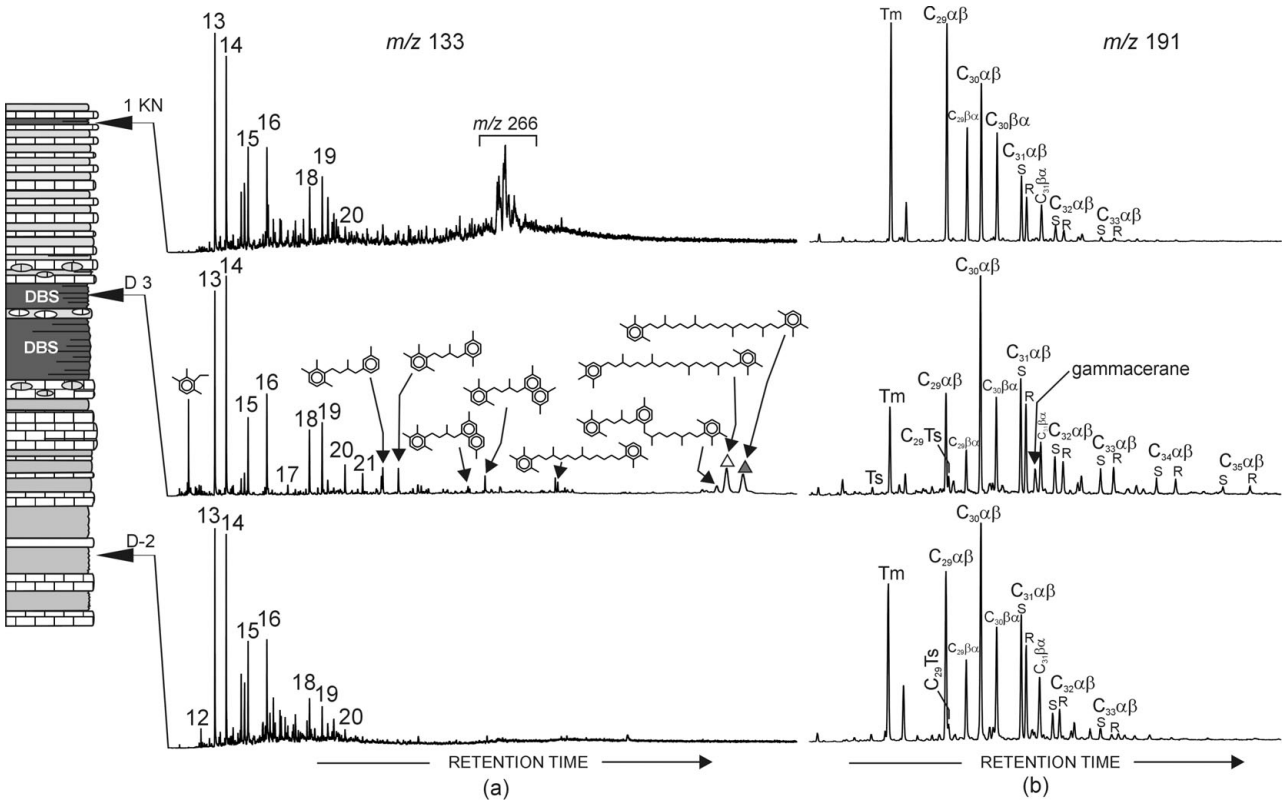

Figure 12. Partial mass chromatogram *m/z* 133 of the three samples from Dasberg section showing the distribution of isorenieratane (filled triangle), 2,3,6-/3,4,5-TM substituted diaryl isoprenoid (open triangle) and their related derivatives including aryl isoprenoids (numbers identify individual carbon number pseudohomologues) in the black shale sample (D3) and lack or trace amount of these compounds in the lower and upper horizons of Dasberg black shale (a) and mass chromatogram *m/z* 191 showing hopanes distribution in the Dasberg samples (b).

to the organic material (Joachimski *et al.* 2001). One exception is the sample D1A, which is partially oxidized/biodegraded with significant participation of the unresolved complex mixture (see Gough, Rhead & Rowland, 1992) and therefore contains lower relative concentrations of *n*-alkanes.

Organic-rich black shales contain gammacerane (Figs 11, 12) in moderate to minor amounts, indicated by the gammacerane/C_{30}-17α-hopane ratio presented in Table 2. Besides black shales, relatively low amounts of gammacerane were detected in grey shale (sample D1), just below the Dasberg shales (Fig. 11). In the organic-poor samples, gammacerane was not detected.

The high abundance of 17α-22,29,30-trisnorhopane (Tm) in comparison to the more thermodynamically stable 18α-22,29,30-trisnorneohopane (Ts) is again consistent with the low maturity of the samples. However, as shown by Bakr & Wilkes (2002), this parameter is strongly dependent on facies influences.

Values of regular sterane to 17α-hopane ratios are lower than 1, but the highest values are observed for the black shales and their intercalation (0.5–0.6, Table 2). Relatively low values of this parameter are rather untypical in the Late Devonian shelf-basin in the Holy Cross Mountains (Marynowski, Narkiewicz & Grelowski, 2000), particularly in the case of organic-rich samples. For example, the values of ster/17α-hop ratio for the Hangenberg shale ranged between 1.5 and 3.8 (Marynowski & Filipiak, 2007). Low values of this parameter may suggest intensive bacterial activity after sedimentation (see Marynowski, Narkiewicz & Grelowski, 2000). However, the highest ster/17α-hop ratio noted in the black shales versus rest of the samples, together with high amounts of AOM affirmed by palynological observations (Fig. 8), implies increased input of algal material and primary productivity during the Dasberg shale deposition.

6.c. Isorenieratane derivatives

Isorenieratane and other diagenetic products of isorenieratene are excellent proxies for the assessment of past photic zone euxinia present in the water column (Summons & Powell, 1986; Sinninghe Damsté & Schouten, 2005; Sinninghe Damsté & Hopmans, 2008) and are usually used as indicators of past sedimentary conditions (e.g. Köster *et al.* 1998; Behrens *et al.* 1998; Pancost *et al.* 1998; Brown & Kenig, 2004; Kenig *et al.* 2004; Grice *et al.* 2005; Marynowski & Filipiak, 2007; Schwab & Spangenberg, 2007; Hays *et al.* 2007; Heimhofer *et al.* 2008).

Two Dasberg black shale samples (D2 and D3) contain isorenieratene derivatives (Figs 11, 12), such as isorenieratane, 2,3,6-/3,4,5-trimethyl-substituted diaryl isoprenoid, 2,3,6-trimethyl-substituted aryl isoprenoids and other diagenetic products of

https://doi.org/10.1017/S0016756809990835 Published online by Cambridge University Press

Table 2. Aryl isoprenoids, isorenieratane, benzo[*a*]anthracene, benzo[*e*]pyrene, benzo[*b*]fluoranthene and sum of pyrolytic PAHs concentrations and molecular parameters based on *n*-alkanes, hopanes, steranes and aryl isoprenoid distributions

Sample	Isorenieratane (μg/g TOC)	Isorenieratane + 2,3,6-/3,4,5- (μg/g TOC)	C_{13}–C_{22} aryl isoprenoids (μg/g TOC)	Gammacerane/ C_{30} 17α-hopane ratio	AIR	Σhop/ Σalk	Ster/ 17α-hop.	B[*a*]A (μg/g TOC)	B[*e*]Py (μg/g TOC)	B[*b*]Fl (μg/g TOC)	Pyrolytic PAHs1 (μg/g TOC]	Pyrolytic PAHs2 (μg/g TOC)
1 KN	0	0	1.7	0	2.93	0.15	0.11	7.85	7.94	23.59	51.92	79.65
2 KN	0	0	0	0	–	0.06	0.27	0.37	2.50	8.70	22.70	24.85
D 4	0	0	4.7	0	0.31	0.08	0.18	0.53	3.20	12.57	37.99	43.01
D 3	32.9	72.9	143.5	0.26	3.09	0.10	0.60	0.77	0.74	1.18	3.18	6.07
D 2A	0	0	3.0	0	0.15	0.12	0.57	0.48	1.60	6.90	14.86	21.73
D 2	22.4	55.9	132.9	0.17	2.41	0.16	0.51	1.03	0.99	1.11	3.77	6.30
D 1A	0	0	1.3	0	0.34	0.60	0.30	0.12	0.36	1.58	3.29	4.88
D 1	0	0	2.5	0.06	1.05	0.26	0.52	0.56	1.31	2.29	5.87	10.58
D 0	0	0	2.6	0	0.53	0.05	0.34	1.02	1.15	2.02	5.77	10.12
D-2	0	0	4.7	0	6.40	0.51	0.37	0.51	2.21	6.29	10.93	22.71
D-3	0	0	3.5	0	2.50	0.35	0.25	0.55	2.04	6.33	9.35	19.55

AIR – Aryl isoprenoid ratio: $(C_{13} - C_{17})/(C_{18} - C_{22})$ (Schwark & Frimmel, 2004)
Ster/17α-hop – regular steranes consist of the C_{27}, C_{28}, C_{29} ααα(20*S* + 20*R*) and αββ(20*S* + 20*R*), 17α-hopanes consist of the C_{29} to C_{33} pseudohomologue (including 22*S* and 22*R* epimers)
Σhop/Σalk – hopanes / *n*-alkanes ratio
B[*a*]A – benzo[*a*]anthracene; B[*e*]Py – benzo[*e*]pyrene; B[*b*]Fl – benzo[*b*]fluoranthene
Pyrolytic PAHs 1 = sum of benzo[*a*]anthracene, benzo[*e*]pyrene, benzo[*a*]pyrene, benzo[*b*]fluoranthene and coronene
Pyrolytic PAHs 2 = sum of fluoranthene, pyrene, benzo[*a*]pyrene, benzo[*b*]fluoranthene, benzo[*ghi*]perylene and coronene (Finkelstein *et al.* 2005)

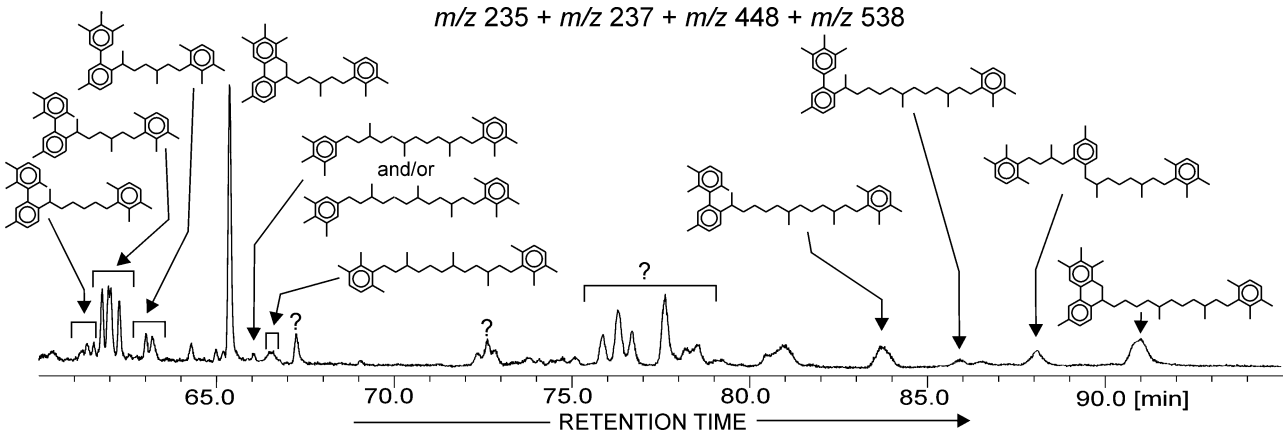

Figure 13. Summed mass chromatogram (*m/z* 235 + 237 + 448 + 538) of the Dasberg black shale sample (D3) showing distribution of long chain dia- and catagenetic products of isorenieratane and 2,3,6/3,4,5-TM substituted diaryl isoprenoid. Identification after Clifford, Clayton & Sinninghe Damsté (1998).

isorenieratene (Figs 12, 13, identified based on Koopmans *et al.* 1996; Clifford, Clayton & Sinninghe Damsté, 1998). These compounds are diagenetic and catagenetic products of strictly anaerobic green sulphur bacteria (*Chlorobiaceae*), which are photosynthetic and require both light and H_2S (Hartgers *et al.* 1994; Koopmans *et al.* 1996). Interestingly, the samples which contain isorenieratane (D2 and D3) also contain gammacerane. This compound is absent in the rest of the sample set, except sample D1 (grey shale), where this compound was detected in low amounts (Table 2). According to Sinninghe Damsté *et al.* (1995), gammacerane is an indicator of water column stratification. This compound is derived from bacterivorous ciliates grazing on bacteria, including green sulphur bacteria, thus it explains the co-occurrence of these compounds in the Dasberg shales.

Similarly, as shown in the Hangenberg section (Marynowski & Filipiak, 2007), differences in the isorenieratane concentration are compatible with differences in the sum of isorenieratane plus 2,3,6-/3,4,5-TM substituted diaryl isoprenoids (Table 2, Fig. 11), suggesting a common origin for both compounds, proposed on the basis of similar $\delta^{13}C$ values (Hartgers *et al.* 1993, 1994). The abundance of aryl isoprenoids in the Dasberg shales and the rest of the samples is variable (Table 2, Figs 11, 12). Two black shale samples are characterized by high concentrations of aryl isoprenoids (Table 2), in contrast to all remaining samples that either do not contain aryl isoprenoids (2KN) or contain a minor amount of these compounds (Table 2). It is notable that values of the aryl isoprenoid ratio (AIR), calculated from the ratio of $C_{13–17}/C_{18–22}$ (Schwark & Frimmel, 2004), are relatively high for black shale samples and low for some organic-poor samples (Table 2). We interpret this phenomenon as being due to the influence of secondary processes such as oxidation and/or water washing on the samples,

https://doi.org/10.1017/S0016756809990835 Published online by Cambridge University Press

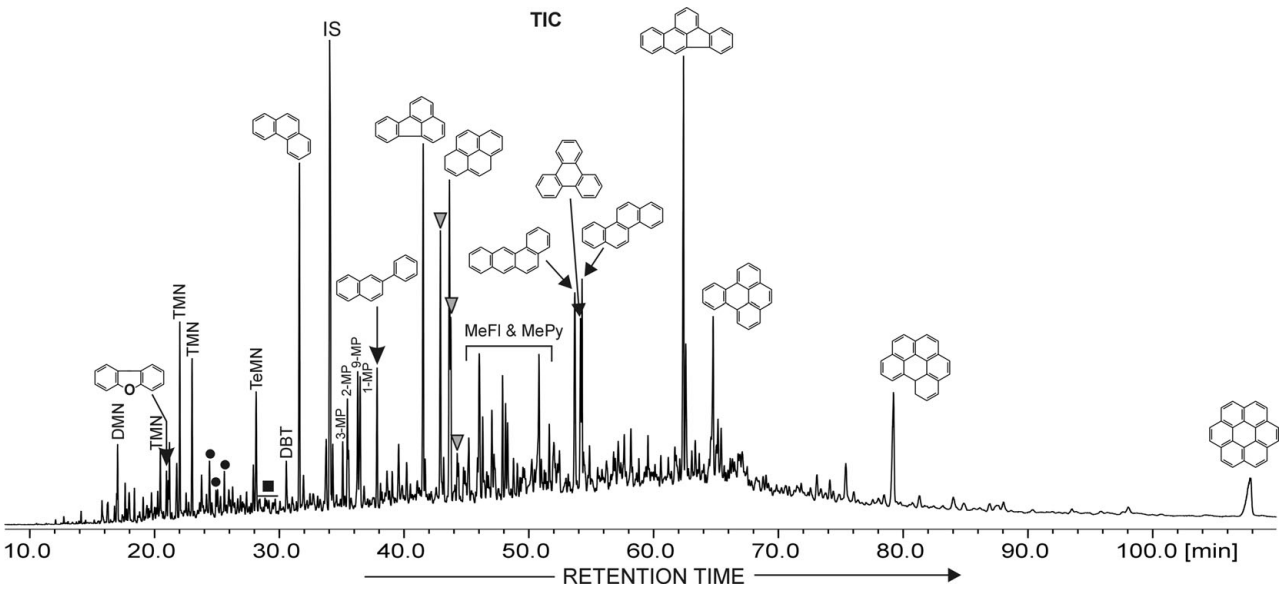

Figure 14. Distribution of total ion chromatogram of an aromatic fraction of the 1KN sample showing high concentration of unsubstituted PAHs. Circles denote methyldibenzofurans, square denote dimethyldibenzofurans, triangles denote benzo[*b*]naphthofuran isomers. DMN – dimethylnaphthalene, TMN – trimethylnaphthalene, TeMN – tetramethylnaphthalene, DBT – dibenzothiophene, MePh – methylphenanthrenes, MePy – methylpyrenes, MeFl – methylfluoranthenes. IS – internal standard. DB-35MS column was used.

causing degradation/dilution of low molecular weight aryl isoprenoids in the organic-poor samples. However, more detailed study is needed to explain this problem.

6.d. Polycyclic aromatic compounds

Samples from the upper part of the section are characterized by the occurrence of high concentrations of unsubstituted polycyclic aromatic hydrocarbons (PAHs) and moderate concentrations of oxygen-containing aromatic compounds (Figs 14, 15). The major identified compounds are: phenanthrene, 2-phenylnaphthalene, fluoranthene, pyrene, benzo[*a*]anthracene, chrysene, triphenylene, benzofluoranthenes, benzo[*a*]pyrene, benzo[*e*]pyrene, indeno[1,2,3-*cd*]pyrene, benzo[*g,h,i*]perylene and coronene (Fig. 14). The same samples contain low to medium concentrations of alkylated derivatives of the above-mentioned structures (Fig. 14), indicating a lack of microbial or sedimentary methylation reactions (e.g. Bastow *et al.* 2000). Such a distribution is characteristic for rapid high-temperature processes, such as combustion, taking place during sedimentation (Venkatesan & Dahl, 1989; Killops & Massoud, 1992; Kruge *et al.* 1994; Jiang *et al.* 1998; Arinobu *et al.* 1999; Finkelstein *et al.* 2005) or hydrothermal petroleum formation at sea-floor spreading centres (Kawka & Simoneit, 1990; Simoneit & Fetzer, 1996).

The concentration of individual polycyclic aromatic hydrocarbons and sum of the pyrolytic PAHs are four to ten times higher in the upper part of the section (samples 1KN, 2KN and D4) than in the remaining section samples (Table 2, Fig. 15). Two different sums of PAHs were calculated: the first proposed by Finkenstein *et al.* (2005) (Table 2, PAHs2) and the second by us in this paper (Table 2, PAHs1). We are using the additional PAH parameter since we believe that in the case of Fammenian samples it better emphasizes the pyrolytic character of organic matter. But in fact, comparison of concentration results for two PAHs parameters are similar for all the samples (Table 2; Fig. 15). Quantitatively, the most important compounds in the sample 1KN, the most enriched in PAHs, are benzo[*b*]fluoranthene (23.6 μg/g TOC), fluoranthene (19.5 μg/g TOC) and pyrene (12.71 μg/g TOC) with somewhat lower concentrations of high molecular weight PAHs (Fig. 14, Table 2). The distribution of aromatic hydrocarbons differs from the Hangenberg section where the high molecular weight, peri-condensed polycyclic aromatic hydrocarbons, for example, coronene, benzo[*g,h,i*]perylene, benzofluoranthenes and benzo[*e*]pyrene, are significantly dominant (Marynowski & Filipiak, 2007). Moreover, in the samples from the Dasberg section, dibenzofuran, methyldibenzofurans, dimethyldibenzofurans and benzo[*b*]naphthofurans were detected (Fig. 14). These oxygen-containing aromatic compounds are most possibly derived from the terrestrial organic matter (Radke, Vriend & Ramanampisoa, 2000; Watson *et al.* 2005; Sephton *et al.* 2005; Wang & Visscher, 2007).

Taking into account the lack of evidence of other PAH sources like ocean spreading centres and active hydrothermal venting in the latest Devonian of the Kowala region, the most likely source for peri-condensed PAH is forest wildfires. As suggested by Grice, Nabbefeld & Maslen (2007), some PAHs, including chrysene, triphenylene and benzo[*e*]pyrene, may have originated from algal OM. However, the co-occurrence of terrestrial OM with undoubtedly identified charcoal fragments (Fig. 9) and PAHs in the

https://doi.org/10.1017/S0016756809990835 Published online by Cambridge University Press

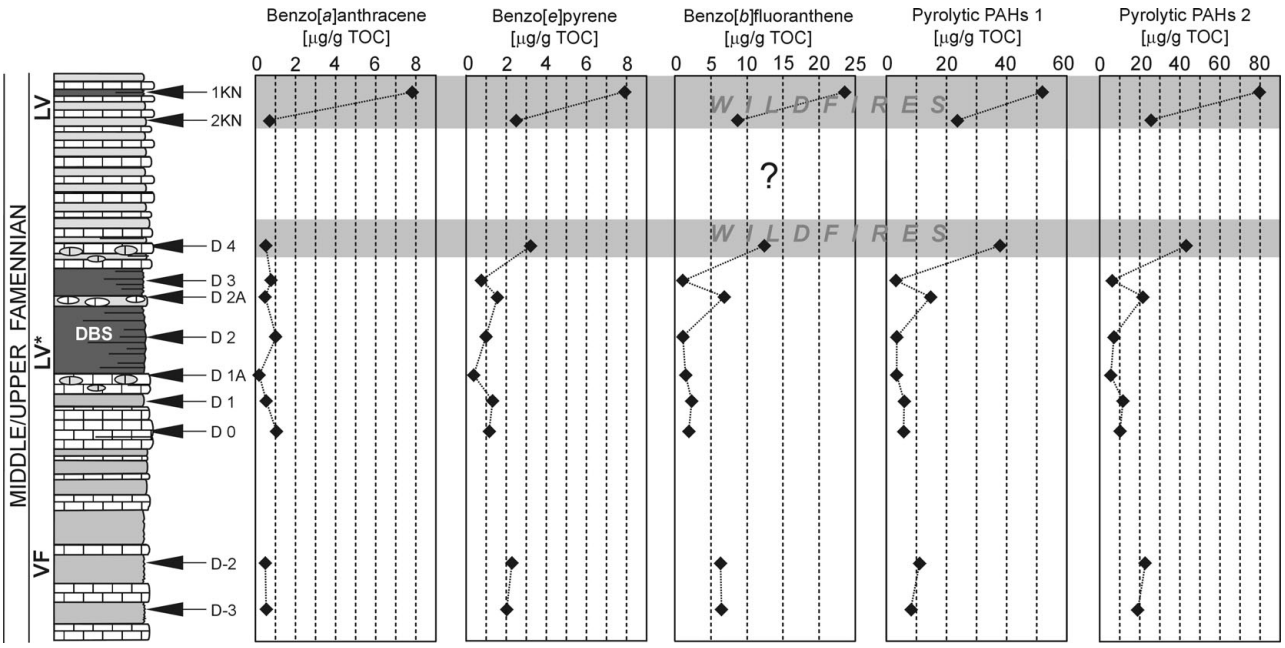

Figure 15. Composite plot of the Dasberg section showing individual and summed PAHs concentrations. For explanation of abbreviations see Table 2.

Dasberg section, as well as relatively high concentrations of the 'true combustion marker' benzo[*a*]pyrene (Grice, Nabbefeld & Maslen, 2007), indicate a wildfire origin for the PAHs. Palynological evidence affirming this interpretation is supplied by the elevated concentration of terrestrial organic debris in samples from the upper part of the section (Figs 8, 9).

7. U/Th ratio

The calculated values of the U/Th ratio range from 0.3 to 1.2 (Fig. 11). In the lower part of the section (samples D-2 and D0), the U/Th ratios (0.77 and 0.8, respectively) point to dysoxic conditions in the bottom environment. Values drop well below 0.75 (0.56 to 0.6) above this (samples D1–D2A, see Fig. 11), indicating a shift to persistent oxygenated bottom waters. However, in sample D3, the highest U/Th value of 1.2 appears, indicating the occurrence of anoxic conditions. Above this level, the U/Th ratios drop again to lower values (0.3 to 0.6), indicating the return of oxygenated bottom water conditions.

Interestingly, the highest U/Th value (1.2) is coincident with the highest values of other organic geochemical parameters that indicate anoxic conditions in the water column (see Fig. 11). On the contrary, below this horizon (during deposition of the shales D2), the U/Th value is very low (0.59) in comparison to other organic geochemical parameters which still indicate water column anoxia (Fig. 11).

8. Pyrite framboid diameter analysis

Pyrite framboids are rather widely scattered in the samples studied. Only in two samples (D2 and D3) was it possible to measure 100 framboids. In the rest of the samples, only 21 to 33 framboids have been measured. The diameters of pyrite framboids vary widely from 1.1 to 22.1 µm, with mean values of 4.0 to 10.6 µm. In all the samples, large framboids (12.0 to 22.1 µm) occur.

Table 3. Uranium (U) and thorium (Th) concentrations, U/Th ratio and pyrite framboid diameter values

Samples	U (ppm)	Th (ppm)	U/Th	Pyrite framboid diameters (µm) n	min	max	mean	sd
1KN	5.6	9.2	0.61	24	5.36	18	9.99	3.16
2KN	2.7	8.6	0.3	–	–	–	–	–
D4	2.5	7.6	0.3	–	–	–	–	–
D3	6.8	5.6	1.2	100	1.1	12	4.01	1.7
D2A	3.5	5.8	0.6	–	–	–	–	–
D2	4.3	7.3	0.59	100	1.62	19.8	5.7	2.4
D1A	3.4	6.2	0.55	–	–	–	–	–
D1	4.2	7.5	0.56	33	4.5	22.1	10.6	4.2
D0	1.2	1.5	0.8					
D-2	5.3	6.9	0.77	21	3.86	21.1	10.6	4.0

n – number of measured framboids, min – minimum value, max – maximum value, mean – mean value, sd – standard deviation.

The lowest two samples (D-2 and D1) and the highest one (1KN) are dominated by large framboids with mean values around 10 µm. Small-sized framboids (< 6 µm), which may have formed in a euxinic water column (see Wilkin, Barnes & Brantley, 1996; Wignall & Newton, 1998), occur as single specimens only (one specimen in samples D-2 and D1, and two specimens in sample 1KN). They have presumably formed within the sediments under an oxic or dysoxic, at most, water column (see Wignall & Newton, 1998). In the samples D2 and D3, on the other hand, the mean values of framboid diameters are the lowest, being 5.7 and 4.0, respectively (Table 3). Furthermore, the standard deviations are the lowest of all the samples investigated, attaining 2.4 and 1.7, respectively. In

https://doi.org/10.1017/S0016756809990835 Published online by Cambridge University Press

sample D2, only a few large framboids above 10 μm are found, and the majority of framboids in that sample are characterized by diameters less than 6 μm. Higher in the section, in sample D3, framboids of less than 4 μm in diameter are most numerous, and the largest framboids, up to 12 μm in diameter, occur as single specimens only. The dominance of small-sized (< 6 μm in diameter) framboids in sample D2 suggests that the anoxic conditions prevailed in the water column, while the presence of a few larger ones may point to a brief oxygenation of the bottom waters. This is also supported by the low value of the U/Th ratio (see Table 3). The framboid diameters (dominance of very small, < 4 μm, specimens and single large framboids only) in sample D3 are in agreement with both the biomarker data and the highest U/Th ratio, which indicate anoxic conditions in the water column and bottom waters, respectively.

9. Discussion

9.a. Productivity and anoxia

The comprehensive application of independent palynological, geochemical and petrographical methods has shown the presence of photic zone anoxia during deposition of the Dasberg black shales in the Kowala section. Although part of the investigated sequence (D-2, D1, 1KN) is characterized by high TOC values, anoxia is only undoubtedly present in the black shale samples (D2 and D3).

All the indices used, such as TOC, isorenieratane and aryl isoprenoid concentrations, gammacerane to hopane ratio, U/Th ratios and the pyrite framboid diameter study indicate that the deepest oxygen deficiency prevailed during sedimentation of the upper Dasberg shale (sample D3; Fig. 11). Anoxic conditions began in the course of the lower Dasberg shale sedimentation (D2) and were interrupted by an oxic episode (sample D2A), as also seen during the somewhat older *Annulata* event, and anoxia reached its maximum during deposition of the upper Dasberg shale.

Our data show that the redox conditions during the deposition of the shales fluctuated.

The presence of green sulphur bacteria biomarkers and dominance of small-sized framboids are indicative of water column anoxia in the photic zone, while the presence of large framboids and low values of the U/Th ratio are characteristic of oxygenated bottom-waters (Tables 2, 3; Fig. 11). Such conflicting data retrieved from a single sample may mean that in fact variable conditions are preserved. Thus, it may be interpreted, that (1) during sedimentation of the lower Dasberg shale (sample D2), the anoxic conditions intermittently occurred in the water column, or (2) the anoxia prevailed in the upper part of the water column, while the bottom waters were oxygenated, at least briefly. Recent findings of oxygen-requiring benthic foraminifera in many Late Devonian black shales of eastern North America (Schieber, 2009) confirm our geochemical observations: despite the presence of anoxia in the water column, the bottom waters were oxygenated.

Somewhat later (sample D2A), anoxic conditions in the water column vanished completely, but during the sedimentation of the upper Dasberg black shales (sample D3), anoxia returned and encompassed both the bottom (high U/Th value and domination of small, < 4 μm, pyrite framboids) and higher part of the water column environments, before another re-oxygenation during the sedimentation of the overlying deposits (Fig. 11).

This model of the Dasberg shale deposition is in agreement with general observations of Late Devonian events, where pulses of anoxia are typically observed (Murphy, Sageman & Hollander, 2000; Racki *et al.* 2002; see Racki, 2005 for review), with the exception of the entirely anoxic upper Dasberg black shale.

As palynological results have shown, both black shale horizons are almost free from acritarchs. Only some stress-indicating 'disaster species' like leiospheres have been found in any abundance. Interestingly, in the sample D3, which was deposited in a completely anoxic environment, *Lophosphaerium* sp. and single *Unellium winslowiae* additionally appear with the common leiosphere taxa. Moreover, acritarchs are present in moderate but constant amounts in the rest of the samples, deposited under oxic conditions. The common presence of AOM in the samples from the DBS also partially supports geochemical results concerning anoxic conditions.

The data obtained enable the interpretation of the sedimentation of the Dasberg black shales as the result of sea-level fluctuations and blooming of primary producers (e.g. Algeo & Scheckler, 1998). A more or less similar situation occurred during sedimentation of the Middle to Upper Frasnian sediments (Marynowski, Filipiak & Pisarzowska, 2008), Kellwasser horizons (Joachimski *et al.* 2001; but see Racki *et al.* 2002), Hangenberg shales (Marynowski & Filipiak, 2007) and Annulata shales (Racka & Marynowski, 2008).

The occurrence of periodically recurrent anoxic events during the Late Devonian may be easily interpreted as multi-stage rapid sea-level rise caused by eustatic pulses (eustatic oscillations) (see Hallam & Wignall, 1999; also Racki, 1998 and Sageman *et al.* 2002). The similarity of particular small- and large-scale Upper Famennian events has already been underlined previously from the viewpoint of ammonoid evolution (Becker, 1993; see also House, 2002), as 'multiphased sudden eustatic and anoxic events...'. Such rapid sea-level changes may have co-occurred with Upper Devonian recurrent periods of global warmth which additionally promoted anoxia due to reduced solubility of oxygen (see Meyer & Kump, 2008).

9.b. Terrestrial organic matter and wildfires

In the upper part of the investigated section the higher PAH concentrations and the presence of small

https://doi.org/10.1017/S0016756809990835 Published online by Cambridge University Press

charcoal particles has been documented, which point to the occurrence of wildfires during sedimentation of these deposits. This is the first evidence of wildfire detected in the vicinity of VF/LV zone boundary. So far, reports on the Upper Famennian wildfires have rarely been correlated with detailed stratigraphical data. The typical marine-basinal character of sedimentation (Szulczewski, 1971; Marynowski, Narkiewicz & Grelowski, 2000) and large amount of charcoal in the samples investigated, suggests that wildfires were common and on a wide-scale.

Charcoal is very buoyant due to its porous structure and therefore capable of prolonged flotation (Batten, 1996). On the other hand, however, during fires, very small pieces of charcoal or ash can be carried high into the atmosphere and then deposited far away from the source. These wind-blown charcoal particles, usually do not exceed 20 μm in diameter (Tyson, 1993; Collinson *et al.* 2007), but a recent report showed that intensive crown fires cause long-distance transport of macroscopic (up to 1.3 cm) charcoal fragments (Tinner *et al.* 2006) (Fig. 9). Moreover, charcoal is not attractive as a food for animals because it is indigestible. Therefore, its concentration in sediments indirectly may be a result of its simple non-digestion, especially in well-oxygenated bottom habitats (e.g. 2KN sample; Fig. 10).

Temperatures of charcoal formation calculated on the basis of inertinite reflectance measurements ranged from 257 to 406 °C, with a mean value of 286 °C. These results suggest that the charcoal was formed in the low-temperature ground and/or surface fires (Scott, 2000; Jones & Lim, 2000). Interestingly, our results differ from those presented by Rimmer, Scott & Cressler (2006), who described 'moderately hot (around 550 °C) fires from the Upper Devonian (Famennian 2c) lowland sites (Red Hill, PA, and Elkins, WV)'. It may suggest that the Upper Devonian charcoal formed during a different wildfire temperature regime.

It is notable that forest wildfire evidence was also found recently for the Hangenberg event horizon from Kowala (Marynowski & Filipiak, 2007). Fairon-Demaret & Hartkopf-Fröder (2004) recognized very well-preserved and strongly taxonomically differentiated charcoalified plant mesofossils in the samples from the Refrath borehole, from the Ardennes-Rhenish Massif (Germany), dated to the LL miospore Zone (*sensu* Maziane, Higgs & Streel, 1999; see also Hartkopf-Fröder, 2004). The frequency of such remains in many samples from over 30 m of the section indicates vegetation that has been rather frequently swept by fire (Fairon-Demaret & Hartkopf-Fröder, 2004). These and the previous reports (Rowe & Jones, 2000; Cressler, 2001; Scott, 2000; Rimmer *et al.* 2004; Rimmer & Scott, 2006; Rimmer, Scott & Cressler, 2006; Scott & Glasspool, 2006; Prestianni *et al.* 2009) provide further evidence of extensive wildfires during Late Famennian times. The main cause of intensive wildfires was a distinct increase of O_2 in the atmosphere, calculated as high as 23 % (Scott & Glasspool, 2006), and the intensive development of land plants including *Archeopteris*, ferns, and some of the earliest seed plants (Rowe & Jones, 2000; Cressler, 2001; Dąbrowska & Filipiak, 2006; Scott & Glasspool, 2006).

Some calculations of the O_2 in the Famennian atmosphere are much lower, showing results from ~ 13 to 15 % (Bergman, Lenton & Watson, 2004; Algeo & Ingall, 2007). However, such values are unrealistic, taking into account the common occurrence of charcoals in the Upper Devonian sediments (see above) and recent burn experiments which undoubtedly showed that the lower O_2 limit for combustion in a natural environment should be increased from 12 to at least 15 % (Belcher & McElwain, 2008).

Moreover, common tuffite intercalations in the Upper Devonian strata (see Marynowski & Filipiak, 2007) suggest strong volcanic activities during this time. Such intensive explosive volcanism could strongly influence the atmospheric acidification, resulting in the formation of miospore tetrads and abnormal miospores found in the uppermost Devonian sediments (Marynowski & Filipiak, 2007).

10. Conclusions

Geochemical proxies reveal the presence of the photic zone anoxia during Dasberg black shales deposition recorded in the Kowala quarry section. The Lower Dasberg black shale sedimentation was characterized by anoxic conditions in the upper part of the water column, but the bottom waters were oxygenated. Throughout deposition of the upper Dasberg black shale, anoxic conditions encompassed both the bottom and water column environments. These dynamically changing redox regimes during sedimentation of the black shales were strictly connected with the sea-level changes, causing enhanced supply of land-derived nutrient remains, and in consequence, blooming of primary marine producers. The palynofacies evolution through the succession suggests a transgression signal corresponding to the IIf sea-level curve *sensu* Johnson, Klapper & Sandberg (1986).

Above the Dasberg black shales, charcoal and elevated concentrations of polycyclic aromatic hydrocarbons were detected, providing evidence of the presence of wildfires just above the boundary of VF/LV palynological zones. Temperatures calculated from the fusinite reflectance values indicate that the charcoal was formed during low-temperature ground and/or surface fires. The high levels of charcoal in the typically marine sedimentary rocks indicate large-scale wildfires and intensive transport of land particles.

Acknowledgements. We are grateful to Professor Grzegorz Racki and Professor Elżbieta Turnau for giving their useful comments and suggestions on the first version of this manuscript. Ewa Teper, M.Sc. (Faculty of Earth Sciences, Sosnowiec) is acknowledged for her help during analyses using ESEM. This work has been financed in part by an MNISW grant: N N307 2379 33 (to LM).

References

ALGEO, T. J. & SCHECKLER, S. E. 1998. Terrestrial-marine teleconnections in the Devonian: links between the evolution of land plants, weathering processes, and marine anoxic events. *Philosophical Transactions of the Royal Society London B* **353**, 113–30.

ALGEO, T. J. & INGALL, E. 2007. Sedimentary Corg:P ratios, paleocean ventilation, and Phanerozoic atmospheric pO_2. *Palaeogeography, Palaeoclimatology, Palaeoecology* **256**, 130–55.

ARINOBU, T., ISHIWATARI, R., KAIHO, K. & LAMOLDA, M. A. 1999. Spike of pyrosynthetic polycyclic aromatic hydrocarbons associated with an abrupt decrease in $\delta^{13}C$ of a terrestrial biomarker at the Cretaceous–Tertiary boundary at Caravaca, Spain. *Geology* **27**, 723–6.

ARMSTROFF, A., WILKES, H., SCHWARZBAUER, J., LITTKE, R. & HORSFIELD, B. 2006. Aromatic hydrocarbon biomarkers in terrestrial organic matter of Devonian to Permian age. *Palaeogeography, Palaeoclimatology, Palaeoecology* **240**, 253–74.

AVKHIMOVITCH, V. I. 1993. Zonation and spore complexes of Devonian and Carboniferous boundary deposits of the Pripyat depression (Byelorussia). *Annales de la Société Géologique de Belgique* **115**, 425–52.

AVKHIMOVITCH, V. I., BYVSHEVA, T. V., HIGGS, K., STREEL, M. & UMNOVA, V. T. 1988. Miospore systematics and stratigraphic correlation of Devonian–Carboniferous Boundary deposits in the European Part of the USRR and western Europe. *Courier Forschungsinstitut Senckenberg* **100**, 169–91.

AVKHIMOVITCH, V. I., TCHIBRIKOVA, E. V., OBUKHOVSKAYA, T. G., NAZARENKO, A. M., UMNOVA, V. T., RASKATOVA, L. G., MANTSOUROVA, V. N., LOBOZIAK, S. & STREEL, M. 1993. Middle and Upper Devonian miospore zonation of Eastern Europe. *Bulletin Des Centres de Recherches Exploration–Production Elf-Aquitaine* **17**, 79–147.

BAKR, M. M. Y. & WILKES, H. 2002. The influence of facies and depositional environment on the occurrence and distribution of carbazoles and benzocarbazoles in crude oils: a case study from the Gulf of Suez, Egypt. *Organic Geochemistry* **33**, 561–80.

BASTOW, T. P., ALEXANDER, R., FISHER, S. J., SINGH, R. K., Van AARSSEN, B. G. K. & KAGI, R. I. 2000. Geosynthesis of organic compounds. Part V – methylation of alkylnaphthalenes. *Organic Geochemistry* **31**, 523–34.

BATTEN, D. J. 1996. Chapter 26A. Palynofacies and palaeoenvironmental interpretation. In *Palynology: principles and applications, Volume 3* (eds J. Jansonius & D. C. McGregor), pp. 1011–64. American Association of Stratigraphic Palynologists Foundation.

BECKER, G., BLESS, M. J. M., STREEL, M. & THOREZ, J. 1974. Palynology and ostracod distribution in the Upper Devonian and basal Dinantian of Belgium and their dependence on sedimentary facies. *Mededelingen, Rijks Geologische Dienst* **25**, 9–99.

BECKER, R. T. 1993. Anoxia, eustatic changes, and Upper Devonian to lowermost Carboniferous global ammonoid diversity. In *The Ammonoidea: Environment, Ecology, and Evolution Change* (ed. M. R. House), pp. 115–63. *Systematics Association Special Volume* **47**. Oxford: Clarendon Press.

BERGMAN, N. M., LENTON, T. M. & WATSON, A. J. 2004. COPSE: a new model of biogeochemical cycling over Phanerozoic time. *American Journal of Science* **304**, 397–437.

BERKOWSKI, B. 2002. Famennian rugosa and heterocorallia from southern Poland. *Palaeontologica Polonica* **61**, 1–87.

BEHRENS, A., WILKES, H., SCHAEFFER, P., CLEGG, H. & ALBRECHT, P. 1998. Molecular characterization of organic matter in sediments from the Keg River formation (Elk Point group), western Canada sedimentary basin. *Organic Geochemistry* **29**, 1905–20.

BELCHER, C. M. & MCELWAIN, J. C. 2008. Limits for combustion in low O_2 redefine paleoatmospheric predictions for the Mesozoic. *Science* **321**, 1197–1200.

BOND, D. & ZATOŃ, M. 2003. Gamma-ray spectrometry across the Upper Devonian basin succession at Kowala in the Holy Cross Mountains (Poland). *Acta Geololgica Pololonica* **53**, 93–9.

BOND, D., WIGNALL, P. B. & RACKI, G. 2004. Extent and duration of marine anoxia during the Frasnian–Famennian (Late Devonian) mass extinction in Poland, Germany, Austria and France. *Geological Magazine* **141**, 173–93.

BOND, D. P. G. & WIGNALL, P. B. 2008. The role of sea-level change and marine anoxia in the Frasnian–Famennian (Late Devonian) mass extinction. *Palaeogeography, Palaeoclimatology, Palaeoecology* **263**, 107–18.

BROWN, T. C. & KENIG, F. 2004. Water column structure during deposition of Middle Devonian – Lower Mississippian black and green/gray shales of the Illinois and Michigan Basin: a biomarker approach. *Palaeogeography, Palaeoclimatology, Palaeoecology* **215**, 59–85.

BYVSHEVA, T. V. 1985. Spores from deposits of the Tournaisian and Visean stages of the Russian Plate. In *Atlas of Spores and Pollen of Phanerozoic Oil and Gas-Bearing Strata of the Russian and Turanian Plates* (eds V. V. Menner & T. V. Byvsheva), pp. 80–158. *Trudy Vsezoiuznogo Nauchno-Issledovatel'skogo Goelogorazvedochnogo Neftianogo Instituta (VNIGRI)* **253** (in Russian).

CAPLAN, M. L. & BUSTIN, M. R. 1999. Devonian–Carboniferous Hangenberg mass extinction event, widespread organic-rich mudrock and anoxia: causes and consequences. *Palaeogeography, Palaeoclimatology, Palaeoecology* **148**, 187–207.

CHOW, N., WENDTE, J. & STASIUK, L. D. 1995. Productivity versus preservation controls on two organic-rich carbonate facies in the Devonian of Alberta: sedimentological and organic petrological evidence. *Bulletin of Canadian Petroleum Geology* **43**, 433–60.

CLIFFORD, D. J., CLAYTON, J. L. & SINNINGHE DAMSTÉ, J. S. 1998. 2,3,6-/3,4,5-Trimethyl substituted diaryl carotenoid derivatives (Chlorobiaceae) in petroleums of the Belarussian Pripyat River Basin. *Organic Geochemistry* **29**, 1253–67.

COLLINSON, M. E., STEART, D. C., SCOTT, A. C., GLASSPOOL, I. J. & HOOKER, J. J. 2007. Episodic fire, runoff and deposition at the Palaeocene–Eocene boundary. *Journal of the Geological Society, London* **164**, 87–97.

COURTINAT, B. 1998. New genera and new species of scolecodonts (fossil annelids) with paleoenvironmental and evolutionary considerations. *Micropaleontology* **44**, 435–40.

CRESSLER, W. L. 2001. Evidence of earliest known wildfires. *Palaios* **16**, 171–4.

DĄBROWSKA, K. & FILIPIAK, P. 2006. The new findings of macroflora from the Famennian of the Holy Cross

Mountains (English summary). *Przegląd Geologiczny* **54**, 720–3.

DEFLANDRE, G. 1945. Microfossiles des calcaires siluriens de la Montagne Noire. *Annales de Paleontologie* **31**, 38–75.

DISNAR, J. R. & HAROUNA, M. 1994. Biological origin of tetracyclic diterpanes, *n*-alkanes and other biomarkers found in Lower Carboniferous Gondwana coals (Niger). *Organic Geochemistry* **21**, 143–52.

DZIK, J. 1997. Emergence and succession of Carboniferous conodont and ammonoid communities in the Polish part of the Variscan sea. *Acta Palaeontologica Polonica* **42**, 57–170.

DZIK, J. 2006. The Famennian 'Golden Age' of conodonts and ammonoids in the Polish part of the Variscan sea. *Palaeontologica Polonica* **63**, 1–360.

ELIE, M., FAURE, P., MICHELS, R., LANDAIS, P. & GRIFFAULT, L. 2000. Natural and laboratory oxidation of low-organic-carbon-content sediments: comparison of chemical changes in hydrocarbons. *Energy & Fuels* **14**, 854–61.

FAIRON-DEMARET, M. & HARTKOPF-FRÖDER, C. 2004. Late Famennian plant mesofossils from the Refrath 1 Borehole (Bergisch Gladbach-Pffrath Syncline; Ardennes-Rhenish Massif, Germany). *Courier Forschungsinstitut Senckenberg* **251**, 89–121.

FILIPIAK, P. 1996. The miospore horizons from the Devonian–Carboniferous boundary beds in the Bolechowice IG 1 borehole (Holy Cross Mountains). *Geological Quarterly* **40**(2), 169–84.

FILIPIAK, P. 2002. Palynofacies around the Frasnian/Famennian boundary in the Holy Cross Mountains, southern Poland. *Palaeogeography, Palaeoclimatology, Palaeoecology* **181**, 313–24.

FILIPIAK, P. 2004. Miospore stratigraphy of Upper Famennian and Lower Carboniferous deposits of the Holy Cross Mountains (central Poland). *Review of Palaeobotany and Palynology* **128**, 291–322.

FILIPIAK, P. 2005. Late Devonian and Early Carboniferous acritarchs and prasinophyta from the Holy Cross Mountains (central Poland). *Review of Palaeobotany and Palynology* **134**, 1–26.

FILIPIAK, P. & RACKI, G. 2005. Unikatowy zapis zdarzeń beztlenowych w profile kamieniołomu Kowala k. Kielc (English summary). *Przegląd Geologiczny* **53**, 846–7.

FINKELSTEIN, D. B., PRATT, L. M., CURTIN, T. M. & BRASSELL, S. C. 2005. Wildfires and seasonal aridity recorded in Late Cretaceous strata from south-eastern Arizona, USA. *Sedimentology* **52**, 587–99.

GONZALEZ, F. 2009. Reappraisal of the organic-walled microphytoplankton genus *Maranhites*: morphology, excystment, and speciation. *Review of Palaeobotany and Palynology* **154**, 6–21.

GOUGH, M. A., RHEAD, M. M. & ROWLAND, S. J. 1992. Biodegradation studies of unresolved complex mixtures of hydrocarbons: model UCM hydrocarbons and the aliphatic UCM. *Organic Geochemistry* **18**, 17–22.

GRICE, K., CAO, C., LOVE, G. D., BÖTTCHER, M. E., TWITCHETT, R. J., GROSJEAN, E., SUMMONS, R. E., TURGEON, S. C., DUNNING, W. & JIN, Y. 2005. Photic zone euxinia during the Permian–Triassic superanoxic event. *Science* **307**, 706–9.

GRICE, K., NABBEFELD, B. & MASLEN, E. 2007. Source and significance of selected polycyclic aromatic hydrocarbons in sediments (Hovea-3 well, Perth Basin, Western Australia) spanning the Permian–Triassic boundary. *Organic Geochemistry* **38**, 1795–1803.

GUY-OHLSON, D. 1996. Chapter 7B. Prasinophycean algae. In *Palynology: principles and applications, Volume 1* (eds J. Jansonius & D. C. McGregor), pp. 181–9. American Association of Stratigraphic Palynologists Foundation.

HABIB, D. & KNAPP, S. D. 1982. Stratigraphic utility of Cretaceous small acritarchs. *Micropaleontology* **28**, 335–71.

HALLAM, A. & WIGNALL, P. B. 1999. Mass extinctions and sea-level changes. *Earth-Science Reviews* **48**, 217–50.

HARTENFELS, S. & BECKER, R. T. In press. Timing of the global Dasberg Event – implications for Famennian eustasy and chronostratigraphy. *Palaeontographica Americana*.

HARTGERS, W. A., SINNINGHE DAMSTÉ, J. S., KOOPMANS, M. P. & DE LEEUW, J. W. 1993. Sedimentary evidence for a diaromatic carotenoid with an unprecedented aromatic-substitution pattern. *Journal of Chemical Society, Chemical Communications* **23**, 1715–16.

HARTGERS, W. A., SINNINGHE DAMSTÉ, J. S., REQUEJO, A. G., ALLAN, J., HAYES, J. M., Yue Ling, Tian-Min Xie, PRIMACK, J. & DE LEEUW, J. W. 1994. A molecular and carbon isotopic study towards the origin and diagenetic fate of diaromatic carotenoids. In *Advances in Organic Geochemistry 1993* (eds N. Telnæs *et al.*), pp. 703–25. *Organic Geochemistry* **22**.

HARTKOPF-FRÖDER, C. 2004. Palynostratigraphy of upper Famennian sediment from the Refrath 1 Borehole (Bergish Gladbach-Paffrath Syncline; Ardennes-Rhenish Massif, Germany). *Courier Forschungsinstitut Senckenberg* **251**, 77–87.

HARTKOPF-FRÖDER, C., KLOPPISCH, M., MANN, U., NEUMANN-MAHLKAU, P., SCHAEFER, R. G. & WILKES, H. 2007. The end-Frasnian mass extinction in the Eifel Mountains, Germany: new insights from organic matter composition and preservation. In *Devonian Events and Correlations* (eds R. T. Becker & W. T. Kirchgasser), pp. 173–96. Geological Society of London, Special Publication no. 278.

HAYS, L. E., BEATTY, T., HENDERSON, C. M., LOVE, G. D. & SUMMONS, R. E. 2007. Evidence for photic zone euxinia through the end-Permian mass extinction in the Panthalassic Ocean (Peace River Basin, Western Canada). *Palaeoworld* **16**, 39–50.

HEIMHOFER, U., HESSELBO, S. P., PANCOST, R. D., MARTILL, D. M., HOCHULI, P. A. & GUZZO, J. V. P. 2008. Evidence for photic-zone euxinia in the Early Albian Santana Formation (Araripe Basin, NE Brazil). *Terra Nova* **20**, 347–54.

HOUSE, M. R. 2002. Strength timing, setting and cause of mid-Palaeozoic extinctions. *Palaeogeography, Palaeoclimatology, Palaeoecology* **181**, 5–25.

JIANG, C., ALEXANDER, R., KAGI, R. I. & MURRAY, A. P. 1998. Polycyclic aromatic hydrocarbons in ancient sediments and their relationship to palaeoclimate. *Organic Geochemistry* **29**, 1721–35.

JOACHIMSKI, M. M., OSTERTAG-HENNING, C., PANCOST, R. D., STRAUSS, H., FREEMAN, K. H., LITTKE, R., SINNINGHE DAMSTÉ, J. S. & RACKI, G. 2001. Water column anoxia, enhanced productivity and concomitant changes in $\delta^{13}C$ and $\delta^{34}S$ across the Frasnian–Famennian boundary (Kowala – Holy Cross Mountains/Poland). *Chemical Geology* **175**, 109–31.

JOHNSON, J. G., KLAPPER, G. & SANDBERG, C. A. 1986. Late Devonian eustatic cycles around margin of Old Red Continent. *Annales de la Société géologique de Belgique* **109**, 141–7.

https://doi.org/10.1017/S0016756809990835 Published online by Cambridge University Press

JONES, T. P. & LIM, B. 2000. Extraterrestrial impacts and wildfires. *Palaeogeography, Palaeoclimatology, Palaeoecology* **164**, 57–66.

KAWKA, O. E. & SIMONEIT, B. R. T. 1990. Polycyclic aromatic hydrocarbons in hydrothermal petroleums from the Guaymas Basin spreading center. *Applied Geochemistry* **5**, 17–27.

KENIG, F., HUDSON, J. D., SINNINGHE DAMSTÉ, J. S. & POPP, B. N. 2004. Intermittent euxinia: Reconciliation of a Jurassic black shale with its biofacies. *Geology* **32**, 421–4.

KILLOPS, S. D. & MASSOUD, M. S. 1992. Polycyclic aromatic hydrocarbons of pyrolytic origin in ancient sediments: evidence for Jurassic vegetation fires. *Organic Geochemistry* **18**, 1–7.

KOOPMANS, M. P., KÖSTER, J., VAN KAAM-PETERS, H. M. E., KENIG, F., SCHOUTEN, S., HARTGERS, W. A., DE LEEUW, J. W. & SINNINGHE DAMSTÉ, J. S. 1996. Diagenetic and catagenetic products of isorenieratane: Molecular indicators for photic zone anoxia. *Geochimica et Cosmochimica Acta* **60**, 4467–96.

KORN, D. 2004. The mid-Famennian ammonoid succession in the Rhenish Mountains: the "*annulata* Event" reconsidered. *Geological Quarterly* **48**, 245–52.

KÖSTER, J., ROSPONDEK, M., SCHOUTEN, S., KOTARBA, M., ZUBRZYCKI, A. & SINNINGHE DAMSTÉ, J. S. 1998. Biomarker geochemistry of a foreland basin: Oligocene Menilite Formation in the Flysch Carpatians of Southeast Poland. In *Advances in Organic Geochemistry 1997* (eds B. Horsfield, M. Radke, R. G. Schaefer & H. Wilkes), pp. 649–69. *Organic Geochemistry* **29**.

KRUGE, M. A., STANKIEWICZ, B. A., CRELLING, J. C., MONTANARI, A. & BENSLEY, D. F. 1994. Fossil charcoal in Cretaceous–Tertiary boundary strata: evidence for catastrophic firestorm and megawave. *Geochimica et Cosmochimica Acta* **58**, 1393–7.

MARYNOWSKI, L., CZECHOWSKI, F. & SIMONEIT, B. R. T. 2001. Phenylnaphthalenes and polyphenyls in Palaeozoic source rocks of the Holy Cross Mountains, Poland. *Organic Geochemistry* **32**, 69–85.

MARYNOWSKI, L. & FILIPIAK, P. 2007. Water column euxinia and wildfire evidence during deposition of the Upper Famennian Hangenberg event horizon from the Holy Cross Mountains (central Poland). *Geological Magazine* **144**, 569–95.

MARYNOWSKI, L., NARKIEWICZ, M. & GRELOWSKI, C. 2000. Biomarkers as environmental indicators in a carbonate complex, example from the Middle to Upper Devonian, Holy Cross Mts., Poland. *Sedimentary Geology* **137**, 187–212.

MARYNOWSKI, L., RAKOCIŃSKI, M. & ZATOŃ, M. 2007. Middle Famennian (Late Devonian) interval with pyritized fauna from the Holy Cross Mountains (Poland): organic geochemistry and pyrite framboid diameter study. *Geochemical Journal* **41**, 187–200.

MARYNOWSKI, L., FILIPIAK, P. & PISARZOWSKA, A. 2008. Organic geochemistry and palynofacies of the Early–Middle Frasnian transition (Late Devonian) of the Holy Cross Mts, southern Poland. *Palaeogeography, Palaeoclimatology, Palaeoecology* **269**, 152–65.

MAZIANE, N., HIGGS, K. T. & STREEL, M. 1999. Revision of late Famennian miospore zonation scheme in eastern Belgium. *Journal of Micropaleontology* **18**, 17–25.

MEYER, K. J. & KUMP, L. R. 2008. Oceanic euxinia in Earth history: causes and consequences. *Annual Review of Earth and Planetary Sciences* **36**, 251–88.

MOREAU-BENOIT, A. 1980. Les spores du Devonien de Libye. *Cahiers de micropaléontologie* **1**, 3–53.

MURPHY, A. E., SAGEMAN, B. B. & HOLLANDER, D. J. 2000. Eutrophication by decoupling of marine biogeochemical cycles of C, N, and P: a mechanism for the Late Gevonian mass extinction. *Geology* **28**, 427–30.

PANCOST, R. D., FREEMAN, K. H., PATZKOWSKY, M. E., WAVREK, D. A. & COLLISTER, J. W. 1998. Molecular indicators of redox and marine photoautotroph composition in the late Middle Ordovician of Iowa, U.S.A. *Organic Geochemistry* **29**, 1649–62.

PETERS, K. E., WALTERS, C. C. & MOLDOWAN, J. M. 2005. *The Biomarker Guide. Vol. 2*. Cambridge University Press, 1155 pp.

PISARZOWSKA, A., SOBSTEL, M. & RACKI, G. 2006. Conodont-based event stratigraphy of the Early–Middle Frasnian transition on South Polish carbonate shelf. *Acta Palaeontologica Polonica* **51**, 609–46.

PLAYFORD, G. 1976. Plant microfossils from the Upper Devonian and Lower Carboniferous of the Canning Basin, Western Australia. *Palaeontographica B* **158B**, 1–71.

PLAYFORD, G. 1977. Lower to Middle Devonian Acritarchs of the Moose River Basin, Ontario. *Geological Survey of Canada, Bulletin* **279**, 1–87.

PLAYFORD, G. & DRING, R. S. 1981. Late Devonian acritarchs from the Carnarvon Basin, Western Australia. *Special Papers in Palaeontology* **27**, 1–78.

PRESTIANNI, C., DECOMBEIX, A.-L., THOREZ, J., FOKAN, D. & GERRIENNE, P. 2009. Famennian charcoal of Belgium. *Palaeogeography, Palaeoclimatology, Palaeoecology* doi:10.1016/j.palaeo.2009.10.008, in press.

RACKA, M. & MARYNOWSKI, L. 2008. Geochemical proxies of the late Famennian *Annulata* event from the Kowala quarry, Holy Cross Mountains, Poland (in Polish). Pierwszy Polski Kongres Geologiczny, June 26–28, 2008. *Abstract, Polskie Towarzystwo Geologiczne, Kraków* **95**.

RACKI, G. 1998. Frasnian–Famennian biotic crisis: undervalued tectonic control? *Palaeogeography, Palaeoclimatology, Palaeoecology* **141**, 177–98.

RACKI, G. 2005. Toward understanding Late Devonian global events: few answers, many questions. In *Understanding Late Devonian and Permian–Triassic Biotic and Climatic Events: Towards an Integrated Approach* (eds D. J. Over, J. R. Morrow & P. B. Wignall), pp. 5–36. Amsterdam: Elsevier.

RACKI, G., RACKA, M., MATYJA, H. & DEVLEESCHOUWER, X. 2002. The Frasnian/Famennian boundary interval in the South Polish–Moravian shelf basins: integrated event-stratigraphical approach. *Palaeogeography, Palaeoclimatology, Palaeoecology* **181**, 251–97.

RADKE, M., VRIEND, S. P. & RAMANAMPISOA, L. R. 2000. Alkyldibenzofurans in terrestrial rocks: Influence of organic facies and maturation. *Geochimica et Cosmochimica Acta* **64**, 275–86.

RAUSCHER, R. 1969. Présence d'une forme nouvelle d'Acritarches dans le Dévonien de Normandie. *Comptes Rendus des Séances de l'Académie Sciences Paris*, série D **268**, 34–6.

RIMMER, S. M., THOMPSON, J. A., GOODNIGHT, S. A. & ROBL, T. L. 2004. Multiple controls on the preservation of organic matter in Devonian–Mississippian marine black shales: geochemical and petrographic evidence. *Palaeogeography, Palaeoclimatology, Palaeoecology* **215**, 125–54.

RIMMER, S. M. & SCOTT, A. C. 2006. Charcoal (inertinite) in Late Devonian marine black shales: Implications

for terrestrial and marine systems and for paleoatmospheric composition. European Geosciences Union General Assembly, April 2–7, 2006, Vienna, Austria, *Geophysical Research Abstracts* **8**, 07972.

RIMMER, S. M., SCOTT, A. C. & CRESSLER, W. L. 2006, Terrestrial-marine linkages: Records of Devonian charcoal, fire, and paleoatmospheric oxygen level. *2006 Annual Meeting Geological Society of America, October 22–25, 2006, Philadelphia, PA, Program with Abstracts* **38**, 341.

ROWE, N. P. & JONES, T. P. 2000. Devonian charcoal. *Palaeogeography, Palaeoclimatology, Palaeoecology* **164**, 331–8.

SAGEMAN, B. B., MURPHY, A. E., WERNE, J. P., VER STRAETEN, CH. A., HOLLANDER, D. J. & LYONS, T. W. 2002. A tale of shales: the relative roles of production, decomposition, and dilution in the accumulation of organic-rich strata, Middle–Upper Devonian, Appalachian basin. *Chemical Geology* **195**, 229–73.

SCHIEBER, J. 2009. Discovery of agglutinated benthic foraminifera in Devonian black shales and their relevance for the redox state of ancient seas. *Palaeogeography, Palaeoclimatology, Palaeoecology* **271**, 292–300.

SCHWAB, V. F. & SPANGENBERG, J. E. 2007. Molecular and isotopic characterization of biomarkers in the Frick Swiss Jura sediments: A palaeoenvironmental reconstruction on the northern Tethys margin. *Organic Geochemistry* **38**, 419–39.

SCHWARK, L. & FRIMMEL, A. 2004. Chemostratigraphy of the Posidonia Black Shale, SW-Germany II. Assessment of extent and persistence of photic-zone anoxia using aryl isoprenoid distribution. *Chemical Geology* **206**, 231–48.

SCOTT, A. C. 2000. The Pre-Quaternary history of fire. *Palaeogeography, Palaeoclimatology, Palaeoecology* **164**, 281–329.

SCOTT, A. C. & GLASSPOOL, I. J. 2006. The diversification of Paleozoic fire systems and fluctuations in atmospheric oxygen concentration. *PNAS* **103**, 10861–5.

SEPHTON, A., LOOY, C. V., BRINKHUIST, H., WIGNALL, P. B., DE LEEUW, J. W. & VISSCHER, H. 2005. Catastrophic soil erosion during the end-Permian biotic crisis. *Geology* **33**, 941–4.

SIMONEIT, B. R. T. & FETZER, J. C. 1996. High molecular weight polycyclic aromatic hydrocarbons in hydrotermal petroleums from the Gulf of California and Northeast Pacific Ocean. *Organic Geochemistry* **24**, 1065–77.

SINNINGHE DAMSTÉ, J. S. & SCHOUTEN, S. 2005. Biological markers for anoxia in the photic zone of the water column. *Handbook of Environmental Chemistry* **2**, 1–37.

SINNINGHE DAMSTÉ, J. S. & HOPMANS, E. C. 2008. Does fossil pigment and DNA data from Mediterranean sediments invalidate the use of green sulfur bacterial pigments and their diagenetic derivatives as proxies for the assessment of past photic zone euxinia? *Environmental Microbiology* **10**, 1392–9.

SINNINGHE DAMSTÉ, J. S., KENIG, F., KOOPMANS, M. P., KÖSTER, J., SCHOUTEN, S., HAYES, J. M. & DE LEEUW, J. W. 1995. Evidence for gammacerane as an indicator of water column stratification. *Geochimica et Cosmochimica Acta* **59**, 1895–1900.

STAPLIN, F. L. 1961. Reef-controlled distribution of Devonian microplancton in Alberta. *Paleontology* **4**(3), 392–424.

STREEL, M., HIGGS, K., LOBOZIAK, S., RIEGEL, W. & STEEMANS, P. 1987. Spore stratigraphy and correlation with faunas and floras in type marine Devonian of the Ardenne-Rhenish region. *Review of Palaeobotany and Palynology* **50**, 211–29.

SUMMERHAYES, C. P. 1987. Organic-rich Cretaceous sediments from the North Atlantic. In *Marine petroleum source rocks* (eds J. Brooks & A. J. Fleet), pp. 301–16. Geological Society of London, Special Publication no. 26.

SUMMONS, R. E. & POWELL, T. G. 1986. Chlorobiaceae in Paleozoic seas revealed by biological markers, isotopes and geology. *Nature* **319**, 763–5.

SZULCZEWSKI, M. 1971. Upper Devonian conodonts, stratigraphy and facial development in the Holy Cross Mts. *Acta Geologica Pololonica* **21**, 1–129.

TAPPAN, H. 1980. *The palaeobiology of plant protists*. San Francisco: W. H. Freeman and Co., 1028 pp.

TAPPAN, H. 1982. Extinction or survival: Selectivity and causes of Phanerozoic crises. *Geological Society of America, Special Paper* **190**, 265–76.

TAPPAN, H. 1986. Phytoplankton: Below the salt at the global table. *Journal of Palaeontology* **60**, 545–54.

TINNER, W., HOFSTETTER, S., ZEUGIN, F., CONEDERA, M., WOHLGEMUTH, T., ZIMMERMAN, L. & ZWEIFEL, R. 2006. Long-distance transport of macroscopic charcoal by an intensive crown fire in the Swiss Alps – implications for fire history reconstruction. *The Holocene* **16**, 287–92.

TRELA, W. & MALEC, J. 2007. Carbon isotope record in sediments of the Devonian–Carboniferous boundary in the southern Holy Cross Mountains. (English summary). *Przegląd Geologiczny* **55**, 411–15.

TURNAU, E. 1975. Micloflora of the Famenian and Tournaisian deposits from boreholes of northern Poland. *Acta Geologica Polonica* **25**, 505–28.

TURNAU, E. 1990. Spore zones of Famennian and Tournaisian deposits from the Kowla 1 borehole. (English summary). *Geological Quarterly* **34**, 291–304.

TYSON, R. V. 1993. Palynofacies analysis. In *Applied micropaleontology* (ed. D. G. Jenkins), pp. 153–91. Kluwer Academic Publishers.

TYSON, R. V. 1995. *Sedimentary Organic Matter. Organic Facies and Palynofacies*. London: Chapman and Hall, 615 pp.

VAN VEEN, P. M. 1981. Aspects of Late Devonian Palynology of Southern Ireland, IV: Morphological variation within *Diducites* a new form genus to accommodate camerate spores with a two layered outer wall. *Review of Palaeobotany and Palynology* **31**, 261–87.

VENKATESAN, M. I. & DAHL, J. 1989. Organic geochemical evidence for global fires at the Cretaceous/Tertiary boundary. *Nature* **338**, 57–60.

WANG, CH. & VISSCHER, H. 2007. Abundance anomalies of aromatic biomarkers in the Permian–Triassic boundary section at Meishan, China – Evidence of end-Permian terrestrial ecosystem collapse. *Palaeogeography, Palaeoclimatology, Palaeoecology* **252**, 291–303.

WATSON, J. S., SEPHTON, M. A., LOOY, C. V. & GILMOUR, I. 2005. Oxygen-containing aromatic compounds in a Late Permian sediment. *Organic Geochemistry* **36**, 371–84.

WICANDER, R. 1974. Upper Devonian–Lower Mississippian acritarchs and prasinophycean algae from Ohio, USA. *Palaeontographica Abteilung B* **148**, 9–43.

WIGNALL, P. B. 1994. *Black shales*. Oxford: Clarendon Press, 127 pp.

WIGNALL, P. B. & NEWTON, R. 1998. Pyrite framboid diameter as a measure of oxygen deficiency in ancient mudrocks. *American Journal of Science* **298**, 537–52.

WILKIN, R. T., BARNES, H. L. & BRANTLEY, S. L. 1996. The size distribution of framboidal pyrite in modern sediments: an indicator of redox conditions. *Geochimica et Cosmochimica Acta* **60**, 3897–912.

YANS, J., CORFIELD, R. M., RACKI, G. & PRÉAT, A. 2007. Evidence for major perturbation of carbon cycle in the middle Frasnian punctata conodont Zone. *Geological Magazine* **144**, 263–70.

ZIEGLER, W. & SANDBERG, C. A. 1990. The Late Devonian Standard Conodont Zonation. *Courier Forschungsinstitut Senckenberg* **121**, 1–115.

ŻAKOWA, H., NEHRING-LEFELD, M. & MALEC, J. 1985. Devonian–Carboniferous boundary in the borehole Kowla 1 (Southern Holy Cross Mts, Poland). Macro- and microfauna. *Geological Quarterly* **33**, 87–95.

https://doi.org/10.1017/S0016756809990835 Published online by Cambridge University Press